

Edge states for the Kalmeyer-Laughlin wave function

Benedikt Herwerth,^{1,*} Germán Sierra,² Hong-Hao Tu,¹ J. Ignacio Cirac,¹ and Anne E. B. Nielsen^{1,3}

¹*Max-Planck-Institut für Quantenoptik, Hans-Kopfermann-Str. 1, D-85748 Garching, Germany*

²*Instituto de Física Teórica, UAM-CSIC, Madrid, Spain*

³*Department of Physics and Astronomy, Aarhus University,
Ny Munkegade 120, DK-8000 Aarhus C, Denmark*

We study lattice wave functions obtained from the $SU(2)_1$ Wess-Zumino-Witten conformal field theory. Following Moore and Read's construction, the Kalmeyer-Laughlin fractional quantum Hall state is defined as a correlation function of primary fields. By an additional insertion of Kac-Moody currents, we associate a wave function to each state of the conformal field theory. These wave functions span the complete Hilbert space of the lattice system. On the cylinder, we study global properties of the lattice states analytically and correlation functions numerically using a Metropolis Monte Carlo method. By comparing short-range bulk correlations, numerical evidence is provided that the states with one current operator represent edge states in the thermodynamic limit. We show that the edge states with one Kac-Moody current of lowest order have a good overlap with low-energy excited states of a local Hamiltonian, for which the Kalmeyer-Laughlin state approximates the ground state. For some states, exact parent Hamiltonians are derived on the cylinder. These Hamiltonians are $SU(2)$ invariant and nonlocal with up to four-body interactions.

PACS numbers: 71.27.+a, 73.43.-f, 11.25.Hf

I. INTRODUCTION

The discovery of the fractional quantum Hall (FQH) effect¹ has revealed the physical existence of a new, strongly correlated state of matter. One surprising property of FQH phases is the fact that they cannot be classified in terms of symmetries². This is a fundamental difference to most other known states of matter and led to the concept of classifying states in terms of topological order^{3,4}. Topological phases are not characterized by a local order parameter but their properties depend on the topology of the system. For example, the ground state degeneracy of a FQH system was shown to depend on the genus of the surface on which the state is defined².

A central characteristic of topological order is the appearance of gapless edge states. Such edge modes are known to be present in a FQH system^{5,6} even though the bulk is gapped. It was shown that these edge states can be used to characterize the topological order of a FQH state^{7,8}. Furthermore, they are of particular physical importance because they determine the transport properties of the system. The strongly correlated state formed by the edge excitations of a FQH system is that of a chiral Luttinger liquid⁷ and its theoretical properties are related to Kac-Moody algebras^{7,9}. For continuous systems, edge state wave functions were constructed as correlation functions of a conformal field theory (CFT)^{10,11} and in terms of Jack polynomials¹².

The use of $1+1$ dimensional CFT in describing FQH states was pioneered by Moore and Read¹³. In this approach, a trial wave function for the FQH state is given as the correlation function of conformal primary fields. Laughlin's wave function for the continuum¹⁴ as well as its $SU(2)$ symmetric, bosonic lattice version, the Kalmeyer-Laughlin (KL) state^{15,16}, were shown to be of this form^{13,17-19}. It was already conjectured by

Moore and Read¹³ that the FQH edge modes should be described by the same CFT that defines the bulk wave function. The idea of this bulk-edge correspondence was later developed into an extension of Moore and Read's method^{10,11}. Within this approach, trial FQH edge states are obtained from CFT descendant states.

This paper is based on a similar ansatz for edge states in lattice systems. Our starting point is the $SU(2)_1$ Wess-Zumino-Witten (WZW) theory, which was used previously^{18,19} to obtain the KL state as a correlation function of primary fields. By insertion of Kac-Moody currents, we define a tower of states, which corresponds to the CFT descendant states. Since we work in a spin formulation, the Hilbert space of the lattice system is that of N spin- $\frac{1}{2}$ degrees of freedom, where occupied sites are represented as spin-up and empty sites as spin-down.

We show that the mapping from CFT states to spin states is surjective, i.e. any state of the spin system can be written as a linear combination of states constructed from the CFT. As a consequence, not all states obtained in this way are edge states. For some of the wave functions, we carry out numerical calculations to test if they describe edge states: On the cylinder, we compare spin correlation functions in the states with one current operator to the KL state using a Metropolis Monte Carlo algorithm^{20,21}. We show that the nearest-neighbor bulk correlations approach each other exponentially as the thermodynamic limit is taken. This indicates that the states with one current operator indeed describe edge states.

In the past years, parent Hamiltonians of the KL state^{18,22-24} and its non-Abelian generalizations²⁴⁻²⁹ were constructed. It was also shown that the KL state³⁰ and non-Abelian FQH lattice states^{26,29} have a good overlap with the ground states of certain local Hamiltonians. For one of these Hamiltonians, an implemen-

tation scheme in ultracold atoms in optical lattices was proposed³⁰. In this work, we study the local Hamiltonians of Ref. 30 on the cylinder and use the KL state and the edge states with one current operator of order one as ansatz states. We find that there is a choice of parameters for which both the ground state and some low-energy excited states have a good overlap with our ansatz states.

Furthermore, we construct Hamiltonians for which the KL state and some of the states obtained from it by insertion of current operators are exact ground states. The proposed parent Hamiltonians are SU(2) invariant and nonlocal with up to four-body interactions.

This paper is structured as follows: In Sec. II, we introduce the CFT model, define the map to a spin- $\frac{1}{2}$ system, and show that it is surjective. In Sec. III, properties of our states on the cylinder are studied and numerical evidence is given that the states with one current operator describe edge states. We consider a local model Hamiltonian in Sec. IV and derive exact parent Hamiltonians for some states on the cylinder in Appendix B. The conclusion is given in Sec. V.

II. CFT MODEL AND SPIN- $\frac{1}{2}$ STATES

In this section, we review some properties of the SU(2)₁ Wess-Zumino-Witten (WZW) theory and define the correspondence between states of the CFT and states of a spin- $\frac{1}{2}$ system on the lattice. It is shown that this map of CFT states to lattice spin states is surjective.

A. SU(2)₁ Wess-Zumino-Witten theory

We consider the chiral sector of the SU(2)₁ WZW theory. In addition to conformal invariance, this theory exhibits an SU(2) symmetry generated by the currents $J^a(z)$ with $a \in \{x, y, z\}$. The modes J_n^a are defined in terms of the Laurent expansion

$$J^a(z) = \sum_{n=-\infty}^{\infty} J_n^a z^{-n-1},$$

$$J_n^a = \oint_0 \frac{dz}{2\pi i} z^n J^a(z), \quad (1)$$

and satisfy the Kac-Moody algebra³¹

$$[J_m^a, J_n^b] = i\varepsilon_{abc} J_{m+n}^c + \frac{m}{2} \delta_{ab} \delta_{m+n,0}. \quad (2)$$

Here, ε_{abc} is the Levi-Civita symbol and δ_{ab} the Kronecker delta. For indices $c \in \{x, y, z\}$, we adopt the convention that indices occurring twice are summed over, unless explicitly stated otherwise.

The SU(2)₁ WZW theory has two primary fields, the identity with conformal weight $h = 0$, and a two-component field $\phi_s(z)$ ($s = \pm 1$) with conformal weight

$h = \frac{1}{4}$. The field $\phi_s(z)$ provides a spin- $\frac{1}{2}$ irreducible representation through its operator product expansion (OPE) with the SU(2) currents³²:

$$J^a(z)\phi_s(w) \sim -\frac{1}{z-w} \sum_{s'=\pm 1} t_{ss'}^a \phi_{s'}(w), \quad (3)$$

where $t^a = \frac{\sigma^a}{2}$ are the SU(2) spin operators.

The field content of the SU(2)₁ WZW theory can be represented in terms of the chiral part $\varphi(z)$ of a free boson field as

$$\phi_s(z) = e^{i\pi(q-1)(s+1)/2} : e^{is\varphi(z)/\sqrt{2}} :,$$

$$J^z(z) = -\frac{i}{\sqrt{2}} \partial_z \phi(z),$$

$$J^\pm(z) = J^x(z) \pm iJ^y(z) = e^{i\pi(q-1)} : e^{\mp i\sqrt{2}\varphi(z)} :. \quad (4)$$

Here, $q = 0$ if the operators act on a state with an even number of modes of the $h = \frac{1}{4}$ primary field and $q = 1$ otherwise, and the colons denote normal ordering. The value of $s \in \{-1, 1\}$ equals two times the spin- z eigenvalue of $\phi_s(z)$.

A general state in the identity sector of the CFT Hilbert space is a linear combination of states

$$(J_{-n_l}^{a_l} \dots J_{-n_1}^{a_1})(0)|0\rangle, \quad (5)$$

where $|0\rangle$ is the CFT vacuum and n_i are positive integers. The sum $k = \sum_{i=1}^l n_i$ defines the level of the state. By means of the Kac-Moody algebra of Eq. (2), a basis can be chosen for which the mode numbers are ordered: $n_l \geq n_{l-1} \geq \dots \geq n_1 > 0$.

B. Spin states on the lattice

To each CFT state $(J_{-n_l}^{a_l} \dots J_{-n_1}^{a_1})(0)|0\rangle$, we associate a state

$$|\psi_{n_l \dots n_1}^{a_l \dots a_1}\rangle = \sum_{s_1, \dots, s_N} \psi_{n_l \dots n_1}^{a_l \dots a_1}(s_1, \dots, s_N) |s_1, \dots, s_N\rangle \quad (6)$$

in the Hilbert space of a system of N spin- $\frac{1}{2}$ degrees of freedom. Its spin wave function is defined as the CFT correlator

$$\psi_{n_l \dots n_1}^{a_l \dots a_1}(s_1, \dots, s_N) = \langle \phi_{s_1}(z_1) \dots \phi_{s_N}(z_N) (J_{-n_l}^{a_l} \dots J_{-n_1}^{a_1})(0) \rangle, \quad (7)$$

where $\langle \dots \rangle$ denotes the expectation value of radially ordered operators in the CFT vacuum.

In the sum of Eq. (6), $s_i = \pm 1$ and $|s_1, \dots, s_N\rangle$ is the tensor product of eigenstates $|s_i\rangle$ of the spin operator t_i^z at position i ($t_i^z |s_i\rangle = \frac{s_i}{2} |s_i\rangle$). The complex coordinates z_i are parameters of the wave function $\psi_{n_l \dots n_1}^{a_l \dots a_1}(s_1, \dots, s_N)$ and define a lattice of positions in the complex plane. Since we want to keep them fixed, we do not explicitly indicate the parametric dependence

of $\psi_{n_1 \dots n_1}^{a_1 \dots a_1}(s_1, \dots, s_N)$ on the positions z_i for simplicity of notation.

The wave function corresponding to the CFT vacuum is given by³²

$$\begin{aligned} \psi_0(s_1, \dots, s_N) &\equiv \langle \phi_{s_1}(z_1) \dots \phi_{s_N}(z_N) \rangle \\ &= \delta_{\mathbf{s}} \chi_{\mathbf{s}} \prod_{i < j}^N (z_i - z_j)^{s_i s_j / 2}, \end{aligned} \quad (8)$$

where $\delta_{\mathbf{s}}$ is 1 if $\sum_{i=1}^N s_i = 0$ and 0 otherwise. $\chi_{\mathbf{s}}$ denotes the Marshall sign factor,

$$\chi_{\mathbf{s}} = \prod_{q=1}^N e^{i\pi(q-1)(s_q+1)/2}. \quad (9)$$

It follows from the alternating sign in the definition of $\phi_s(z)$ [cf. Eq. (4)]. Due to the presence of the Marshall sign factor, the state ψ_0 is a singlet of the total spin²⁷ $T^a = \sum_{i=1}^N t_i^a$:

$$T^a |\psi_0\rangle = 0. \quad (10)$$

We assume that N is even, as required by the charge neutrality condition $\sum_{i=1}^N s_i = 0$ in the wave function of ψ_0 . It was shown previously that ψ_0 is equivalent to the KL state^{17,18}. We note that the wave function ψ_0 of Eq. (8) contains a square root, which has two branches. It is assumed that the same branch is taken for all factors in Eq. (8). Which of the two branches is chosen is not important, since this choice only influences the wave function by a total factor.

The states $\psi_{n_1 \dots n_1}^{a_1 \dots a_1}$ can be related to ψ_0 by an application of spin operators³³: In Eq. (7), one can write the modes $J_{-n_i}^{a_i}$ as an integral according to Eq. (1), deform the integral contour, and apply the OPE (3) between current operators and primary fields. Defining

$$u_k^a \equiv \sum_{i=1}^N (z_i)^k t_i^a \quad (11)$$

it then follows that

$$|\psi_{n_1 \dots n_1}^{a_1 \dots a_1}\rangle = u_{-n_1}^{a_1} \dots u_{-n_1}^{a_1} |\psi_0\rangle. \quad (12)$$

We note that the operators u_k^a defined in Eq. (11) satisfy

$$[u_m^a, u_n^b] = i\varepsilon_{abc} u_{m+n}^c, \quad (13)$$

which is a Kac-Moody algebra with vanishing central extension.

In addition to the states $\psi_{n_1 \dots n_1}^{a_1 \dots a_1}$, we also consider the wave functions obtained by the insertion of two additional primary fields, one at $z_0 = 0$ and one at $z_\infty = \infty$:

$$\begin{aligned} &\psi_0^{s_0, s_\infty}(s_1, \dots, s_N) \\ &\equiv \langle \phi_{s_\infty}(\infty) \phi_{s_1}(z_1) \dots \phi_{s_N}(z_N) \phi_{s_0}(0) \rangle \\ &\propto \delta_{\mathbf{s}} \chi_{\mathbf{s}} (-1)^{(1-s_\infty)/2} \prod_{n=1}^N z_n^{s_0 s_n / 2} \prod_{n < m}^N (z_n - z_m)^{s_n s_m / 2}, \end{aligned} \quad (14)$$

where $\delta_{\mathbf{s}}$ is 1 if $s_0 + s_\infty + \sum_{j=1}^N s_j = 0$ and 0 otherwise. The state $\psi_0^{s_0, s_\infty}$ contains a singlet and a triplet obtained by the tensor product decomposition of the two additional spin- $\frac{1}{2}$ fields. As we show in Sec. IIIB, the singlet component on the cylinder can be derived from the wave function of N primary fields on a torus in the limit where the torus becomes a cylinder.

We note that the states ψ_0 , $\psi_{n_1 \dots n_1}^{a_1 \dots a_1}$, and $\psi_0^{s_0, s_\infty}$ of Eqs. (7, 8), and (14) are not normalized. Whenever the norm of a state is needed, it will be explicitly included in the corresponding expression.

C. Completeness of spin states

One may ask if the linear transformation that maps CFT states $(J_{-n_1}^{a_1} \dots J_{-n_1}^{a_1})(0)|0\rangle$ to spin states $\psi_{n_1 \dots n_1}^{a_1 \dots a_1}$ is surjective, i.e. whether any state in the Hilbert space \mathcal{H}_N of N spin- $\frac{1}{2}$ particles can be written as a linear combination of the states $\psi_{n_1 \dots n_1}^{a_1 \dots a_1}$. We now show that this is indeed the case. Introducing the $N \times N$ matrix

$$\mathcal{Z} = \begin{pmatrix} 1 & \dots & 1 \\ (z_1)^{-1} & \dots & (z_N)^{-1} \\ (z_1)^{-2} & \dots & (z_N)^{-2} \\ \vdots & \vdots & \vdots \\ (z_1)^{-(N-1)} & \dots & (z_N)^{-(N-1)} \end{pmatrix}, \quad (15)$$

the definition of Eq. (11) becomes

$$\begin{pmatrix} u_0^a \\ u_{-1}^a \\ \vdots \\ u_{-(N-1)}^a \end{pmatrix} = \mathcal{Z} \begin{pmatrix} t_1^a \\ t_2^a \\ \vdots \\ t_N^a \end{pmatrix}. \quad (16)$$

The determinant of \mathcal{Z} is the well known Vandermonde determinant:

$$\det(\mathcal{Z}) = \prod_{i < j}^N (z_j^{-1} - z_i^{-1}). \quad (17)$$

\mathcal{Z} is therefore nonsingular if all positions z_i are distinct, which we assume to be the case. As a consequence, the relation of Eq. (16) can be inverted, i.e. all spin operators t_j^a can be written as linear combinations of u_{-n}^a with $n \in \{0, \dots, N-1\}$.

The Hilbert space \mathcal{H}_N is spanned by the states obtained from any nonzero state by successive application of spin operators t_i^a . Given that t_i^a can be expressed in terms of u_{-n}^a , it follows in particular that the states $|\psi_{n_1 \dots n_1}^{a_1 \dots a_1}\rangle = u_{-n_1}^{a_1} \dots u_{-n_1}^{a_1} |\psi_0\rangle$ with $n_i \in \{0, \dots, N-1\}$ span \mathcal{H}_N . Since ψ_0 is a singlet and $u_0^a = \sum_{j=1}^N t_j^a$ is the total spin, a state

$$u_0^a u_{-n_1}^{a_1} \dots u_{-n_1}^{a_1} |\psi_0\rangle \quad (18)$$

can be written in terms of states for which all mode numbers are greater than zero by commuting u_0^a to the right

until it annihilates ψ_0 [cf. the commutator of Eq. (13)]. Therefore, \mathcal{H}_N is spanned by the states $\psi_{n_1 \dots n_1}^{a_1 \dots a_1}$ with $n_i > 0$.

This argument shows that not all states constructed by the insertion of current operators can be edge states compared to ψ_0 . For the states with one current operator J_n^a , numerical evidence will be given in Sec. III C that these represent edge states on the cylinder.

The fact that the states $\psi_{n_1 \dots n_1}^{a_1 \dots a_1}$ span \mathcal{H}_N raises the question about the minimal level $k = \sum_{j=1}^l n_j$ needed to obtain the complete Hilbert space. We note that an upper bound is given by $k = N(N-1)$, since any product of spin operators t_i^a can be reduced to a product of at most N spin operators. Each of these spin operators can then be expanded in terms of the operators u_{-n}^a with $n \in \{0, \dots, N-1\}$. We carried out numerical calculations for the states $\psi_{n_1 \dots n_1}^{a_1 \dots a_1}$ which indicate that the states up to level $k = (N/2)^2$ are enough to obtain the complete Hilbert space from ψ_0 .

III. PROPERTIES OF STATES ON THE CYLINDER

In this section, we study properties of the states defined in Sec. II B on the cylinder.

We consider a square lattice with N_x lattice sites in the open direction and N_y lattice sites in the periodical direction of the cylinder. After mapping the cylinder to the complex plane, the coordinates assume the form

$$z_j = e^{\frac{2\pi}{N_y}(j_x + i j_y)} e^{-\frac{2\pi}{N_y} \frac{N_x + 1}{2}}. \quad (19)$$

Here, $j_x \in \{1, \dots, N_x\}$ is the x -component of the index and $j_y \in \{1, \dots, N_y\}$ is the y -component, so that $j = (j_x - 1)N_y + j_y$ ranges from 1 to $N = N_x N_y$. For the remainder of this paper, we adopt a two-index notation, where this is convenient, i.e. we may write z_{j_x, j_y} instead of z_j , denoting the x - and y -components by subscripts.

Note that one has the freedom to rescale the coordinates since this changes the wave functions only by a total factor. The constant factor that we included in Eq. (19) is chosen such that the center of the cylinder is at the unit circle.

We assume that the number of sites N is even. It is also possible to study the case of N being odd which will show the existence of two topological sectors. However, we can already identify the two anyonic sectors for N even. As will be shown below in Sec. III B, the state ψ_0 and the singlet component ψ_0^{sgl} of the state with two additional spins (one at $z_0 = 0$ and one at $z_\infty = \infty$) can be obtained from the wave function of N primary fields on the torus in the limit where the torus becomes a cylinder. This argumentation shows that the two states ψ_0 and ψ_0^{sgl} represent the two anyonic sectors in the case of an even number of spins. It would be possible to consider an odd number of sites on the cylinder by putting an additional spin either at $z_0 = 0$ or at $z_\infty = \infty$ so that

the charge neutrality condition is satisfied. On the torus, however, such a construction is not possible and the argumentation that we used to identify the two sectors for even N does not directly apply.

A. Global transformation properties of CFT states

In this subsection, we study global transformation properties of the states ψ_0 , $\psi_{n_1 \dots n_1}^{a_1 \dots a_1}$, and $\psi_0^{s_0, s_\infty}$. This serves two purposes: First, it allows us to conclude that states with a different momentum are orthogonal, i.e. they have different global properties. Later, we will study their local behavior numerically and compare spin correlation functions in the bulk. The symmetries derived in this subsection will be exploited in our numerical calculations to obtain efficient Monte Carlo estimates.

We consider the translation operator in the periodical direction \mathcal{T}_y and the inversion operator \mathcal{I} . Their precise definition and the derivation of their action on the states ψ_0 , $\psi_{n_1 \dots n_1}^{a_1 \dots a_1}$, and $\psi_0^{s_0, s_\infty}$ are given in Appendix A. Geometrically, the translation operator rotates the system in the periodical direction and the inversion operator corresponds to a reflection of the cylinder along its two central cross sections. We call it an inversion because it acts on the coordinates defined in Eq. (19) as $z_i \rightarrow z_i^{-1}$.

Eigenstates of \mathcal{T}_y and \mathcal{I} are given in Table I. As we show in Appendix A 3, applying the inversion \mathcal{I} to $\psi_{n_1 \dots n_1}^{a_1 \dots a_1}$ corresponds to inserting the current operators at $z_\infty = \infty$ instead of $z_0 = 0$. We use the notation $\psi_{-n_1 \dots -n_1}^{a_1 \dots a_1}$ for these states:

$$\begin{aligned} \psi_{-n_1 \dots -n_1}^{a_1 \dots a_1}(s_1, \dots, s_N) \\ &\equiv \langle J_{n_1}^{a_1} \dots J_{n_1}^{a_1} \phi_{s_1}(z_1) \dots \phi_{s_N}(z_1) \rangle \\ &= (u_{n_1}^{a_1} \dots u_{n_1}^{a_1} \psi_0)(s_1, \dots, s_N). \end{aligned} \quad (20)$$

Since the momentum in the periodical direction P_y is related to \mathcal{T}_y through the relation $\mathcal{T}_y = e^{iP_y}$, we conclude from Table I that an additional insertion of a current operator J_n^a into the correlation function of primary fields adds a momentum of $-2\pi n/N_y$ to the state. In particular, the states ψ_0 and $\psi_{n_1 \dots n_1}^{a_1 \dots a_1}$ have a different momentum if $k = \sum_{j=1}^l n_j$ is different from 0 modulo N_y .

B. Relation to the KL states on the torus

In this subsection, we place the system on the torus and take a limit in which the torus becomes a cylinder. We show that the wave function of N primary fields on the torus gives rise to ψ_0 and the singlet component ψ_0^{sgl} of $\psi_0^{s_0, s_\infty}$ on the cylinder.

We define the torus for $\omega_1 > 0$ and $\omega_2 = iL$ with $L > 0$ by identifying a complex number z with $z + n\omega_1 + m\omega_2$ for $m, n \in \mathbb{Z}$. The two circumferences of the torus are therefore given by ω_1 and $|\omega_2|$. Let us denote the positions on the torus by v_i , i.e. we assume that v_i lie in the rectangle spanned by ω_1 and ω_2 . Keeping the positions v_i fixed

TABLE I. Eigenstates of the translation operator \mathcal{T}_y and the inversion \mathcal{I} . The sum of mode numbers $\sum_{j=1}^l n_j$ is denoted by k . For the states $\psi_{-n_l \dots -n_1}^{a_l \dots a_1}$, the current operators are inserted at $z_\infty = \infty$ [cf. Eq. (20)].

Eigenstate	\mathcal{T}_y	\mathcal{I}
ψ_0	$(-1)^{N_x \frac{N}{2}}$	$(-1)^{N_y \frac{N}{2}}$
$\psi_{n_l \dots n_1}^{a_l \dots a_1}$	$(-1)^{N_x \frac{N}{2}} e^{-\frac{2\pi i}{N_y} k}$	—
$\psi_{n_l \dots n_1}^{a_l \dots a_1} \pm \psi_{-n_l \dots -n_1}^{a_l \dots a_1}$	—	$(\pm 1)(-1)^{N_y \frac{N}{2}}$
$\psi_0^{s_0, s_\infty}$	$(-1)^{N_x \frac{N}{2} + N_x}$	—
$\psi_0^{\uparrow, \downarrow} - \psi_0^{\downarrow, \uparrow}$	$(-1)^{N_x \frac{N}{2} + N_x}$	$(-1)^{N_y \frac{N}{2} + N_x}$
$\psi_0^{\uparrow, \uparrow}, \psi_0^{\uparrow, \downarrow} + \psi_0^{\downarrow, \uparrow}$, and $\psi_0^{\downarrow, \downarrow}$	$(-1)^{N_x \frac{N}{2} + N_x}$	$(-1)^{N_y \frac{N}{2} + N_x + 1}$

and taking the circumference $L = |\omega_2| \rightarrow \infty$ transforms the torus into a cylinder, as illustrated in Fig. 1.

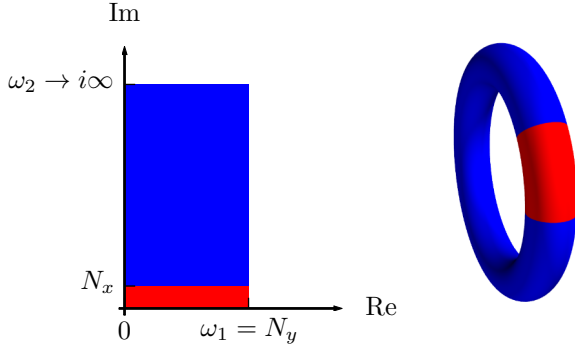


FIG. 1. (Color online) Limit in which the torus becomes a cylinder: The circumference $|\omega_2|$ is taken to infinity while the positions lie in the finite region of size $N_x \times N_y$ (red patch).

On the torus, there are two states ψ_k^{torus} with $k \in \{0, \frac{1}{2}\}$. These are given by¹⁹

$$\begin{aligned} \psi_k^{\text{torus}}(s_1, \dots, s_N) &= \langle \phi_{s_1}(v_1) \dots \phi_{s_N}(v_N) \rangle_k \\ &\propto \delta_{\mathbf{s}} \chi_{\mathbf{s}} \theta \begin{bmatrix} k \\ 0 \end{bmatrix} \left(\sum_{i=1}^N \zeta_i s_i, 2\tau \right) \prod_{i < j}^N \left(\theta \begin{bmatrix} \frac{1}{2} \\ \frac{1}{2} \end{bmatrix} (\zeta_i - \zeta_j, \tau) \right)^{s_i s_j / 2}. \end{aligned} \quad (21)$$

Here, $\zeta_i = v_i / \omega_1$ are the rescaled positions, $\tau = \omega_2 / \omega_1$ is the modular parameter of the torus, and θ the Riemann theta function defined as

$$\theta \begin{bmatrix} a \\ b \end{bmatrix} (\zeta, \tau) = \sum_{n \in \mathbb{Z}} e^{i\pi\tau(n+a)^2 + 2\pi i(n+a)(\zeta+b)}. \quad (22)$$

The limit $\omega_2 \rightarrow i\infty$, which transforms the torus into a cylinder, implies $\tau \rightarrow i\infty$. In this case, only the terms with the smallest value of $(n+a)^2$ contribute to the sum of Eq. (22). These terms have $n = 0$ for $a = 0$ and

$n \in \{-1, 0\}$ for $a = \frac{1}{2}$. Therefore,

$$\begin{aligned} \theta \begin{bmatrix} 0 \\ 0 \end{bmatrix} (\zeta, 2\tau) &\rightarrow 1, \\ \theta \begin{bmatrix} \frac{1}{2} \\ 0 \end{bmatrix} (\zeta, 2\tau) &\rightarrow e^{\frac{\pi i \tau}{2}} (e^{i\pi\zeta} + e^{-i\pi\zeta}), \quad \text{and} \\ \theta \begin{bmatrix} \frac{1}{2} \\ \frac{1}{2} \end{bmatrix} (\zeta_i - \zeta_j, \tau) &\rightarrow i e^{-i\pi(\zeta_i + \zeta_j)} e^{\frac{i\pi\tau}{4}} (e^{2\pi i \zeta_i} - e^{2\pi i \zeta_j}), \end{aligned} \quad (23)$$

for $\tau \rightarrow i\infty$. With $\sum_{j=1}^N s_j = 0$, it follows that

$$\prod_{m < n}^N e^{-i\frac{\pi}{2}(\zeta_m + \zeta_n)s_m s_n} = e^{i\frac{\pi}{2} \sum_{n=1}^N \zeta_n}. \quad (24)$$

In the limit $\omega_2 \rightarrow i\infty$, we therefore obtain

$$\begin{aligned} \psi_0^{\text{torus}}(s_1, \dots, s_N) \\ \propto \delta_{\mathbf{s}} \chi_{\mathbf{s}} \prod_{m < n}^N \left(e^{2\pi i v_m / \omega_1} - e^{2\pi i v_n / \omega_1} \right)^{s_m s_n / 2} \end{aligned} \quad (25)$$

and

$$\begin{aligned} \psi_{\frac{1}{2}}^{\text{torus}}(s_1, \dots, s_N) \\ \propto \delta_{\mathbf{s}} \chi_{\mathbf{s}} \left(\prod_{n=1}^N e^{\pi i v_n s_n / \omega_1} + \prod_{n=1}^N e^{-\pi i v_n s_n / \omega_1} \right) \\ \times \prod_{m < n}^N \left(e^{2\pi i v_m / \omega_1} - e^{2\pi i v_n / \omega_1} \right)^{s_m s_n / 2}. \end{aligned} \quad (26)$$

The exponentials $e^{2\pi i v_n / \omega_1}$ lie on a cylinder of circumference ω_1 . We therefore identify $z_n = e^{2\pi i v_n / \omega_1}$ and $N_y = \omega_1$. Comparing the expressions for ψ_k^{torus} in the limit $\omega_2 \rightarrow \infty$ to Eqs. (8) and (14), we conclude that $\psi_0^{\text{torus}} \propto \psi_0$ and $\psi_{\frac{1}{2}}^{\text{torus}} \propto \psi_0^{\uparrow, \downarrow} - \psi_0^{\downarrow, \uparrow} \equiv \psi_0^{\text{sgl}}$.

It would be very interesting to investigate the relation between excited states in one and two dimensions on the circle and the plane, respectively, to those on the torus. The result for the relation between $\psi_{\frac{1}{2}}^{\text{torus}}$ and ψ_0^{sgl} is a first step in that direction.

C. Spin correlation functions and edge states

We calculated two-point spin correlation functions in the states ψ_0 , ψ_1^a and in the singlet state

$$\psi_0^{\text{sgl}} \equiv \psi_0^{\uparrow, \downarrow} - \psi_0^{\downarrow, \uparrow} \quad (27)$$

using a Metropolis Monte Carlo algorithm. This allowed us to compare properties of the states numerically for large system sizes by sampling the relevant probability distributions. We furthermore exploited the translation and inversion symmetries of Table I to average over

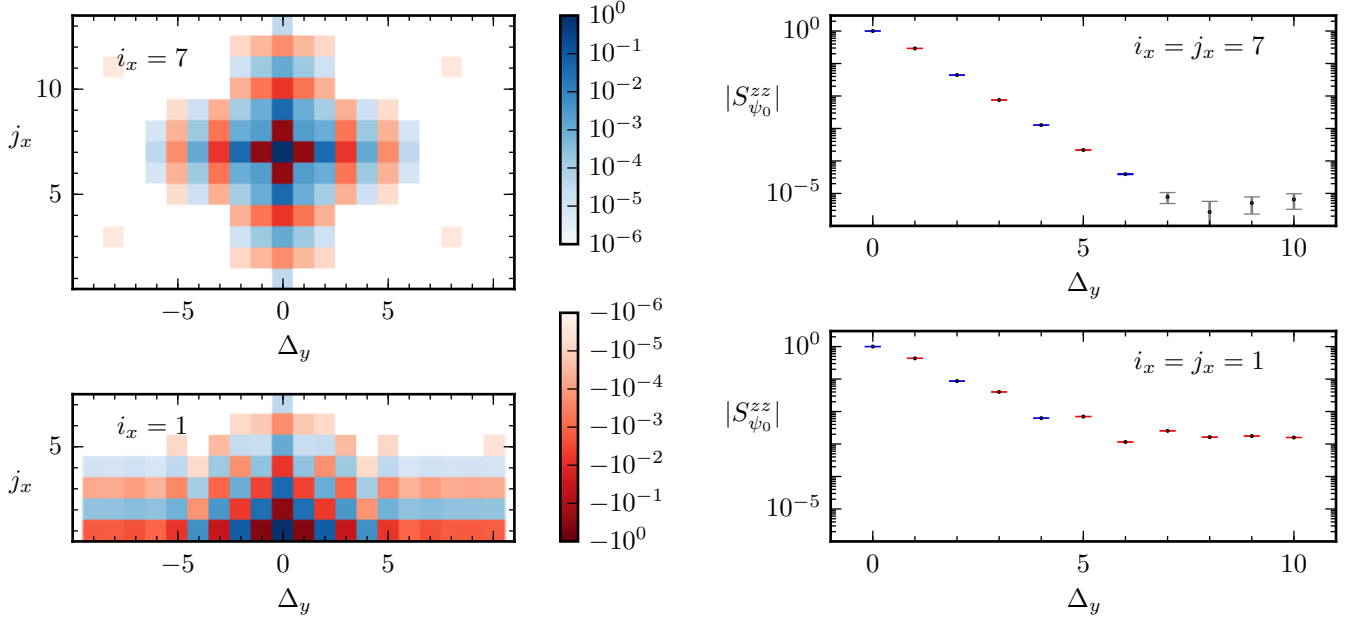


FIG. 2. (Color online) Two-point spin correlation function $S_{\psi_0}^{zz}(i_x, j_x, \Delta_y)$ in the bulk (upper panels) and at the edge (lower panels) for $N_x = 13$ and $N_y = 20$. The left panels show the two-dimensional dependency in a color plot. Whenever the value of the correlation function does not differ from zero by more than three times the estimated error, we excluded the data point from the plot (blank fields). In the right panels, the absolute value $|S_{\psi_0}^{zz}(i_x, i_x, \Delta_y)|$ of the correlation function along the y -direction is plotted. Points for which the sign of the correlation function is positive (negative) are shown in blue (red). For the data shown in gray, the mean value does not differ from zero by more than three times the estimated error. In the bulk, the correlations decay exponentially, while a nonzero, negative correlation remains at the edge for $\Delta_y \geq 5$.

equivalent correlation functions, thus obtaining a faster converging Monte Carlo estimate.

In this subsection, we shall use the notation

$$S_{\psi}^{ab}(i_x, j_x, \Delta_y) = 4 \frac{\langle \psi | t_{i_x, \Delta_y+1}^a t_{j_x, 1}^b | \psi \rangle}{\langle \psi | \psi \rangle} \quad (28)$$

for the two-point correlation function in a state ψ . Since all wave functions that we consider have a translational symmetry in the periodical direction, their value only depends on the difference Δ_y of the positions in the y -direction.

Before comparing the wave functions with each other, we discuss the spin ordering pattern in ψ_0 , which is encoded in the correlation function $S_{\psi_0}^{zz}(i_x, j_x, \Delta_y)$. (Since ψ_0 is a singlet, xx -, yy - and zz -correlations are the same and only correlation functions with $a = b$ are nonzero.) Our numerical results are shown in Fig. 2. In the bulk of the system, we observe a ring-like structure with an alternating magnetization. At the edge, the correlations are anti-ferromagnetic at short distances. At larger distances along the y -direction, however, the sign becomes stationary and a negative correlation remains. In the two-dimensional picture, the ordering is still characterized by an alternating magnetization with the sign of the correlation function changing along the x -direction.

We now discuss the question if the states ψ_1^a can be considered as edge states. If so, then the local properties of ψ_1^a and ψ_0 in the bulk should be the same. Since these

are encoded in the spin correlation functions, we compared the nearest-neighbor two-point correlators in the bulk for different system sizes. The relative differences

$$\left| \frac{S_{\psi_1^a}^{bc}(i_x, j_x, \Delta_y) - S_{\psi_0}^{bc}(i_x, j_x, \Delta_y)}{S_{\psi_0}^{bc}(i_x, j_x, \Delta_y)} \right| \quad (29)$$

are shown in Fig. 3 for $a = b = c = z$ (left panels) and $a = z, b = c = x$ (right panels). Correlation functions for other choices of a, b , and c either vanish or can be reduced to these due to the $SU(2)$ invariance of ψ_0 . In the upper panels, the correlations along the y -direction are shown and in the panels of the lower two rows along the x -direction. We find that the relative differences approach zero exponentially as a function of N_x . Even though the differences tend to be larger for smaller N_y , they are still exponentially suppressed as N_x is increased. This is an indication that the wave functions ψ_1^a indeed describe edge states compared to ψ_0 as the thermodynamic limit in the open direction is taken.

Our results for the comparison between ψ_0^{sgl} and ψ_0 are shown in Fig. 4. Since both ψ_0 and ψ_0^{sgl} are singlets, it is enough to compare the zz -correlations. Furthermore, the correlations in the positive and the negative x -direction are the same in the middle of the cylinder since ψ_0 and ψ_0^{sgl} are symmetric under the inversion, cf. Sec. III A. In contrast to ψ_1^a , we find that the thermodynamic limit in the x -direction is not enough for the differences to

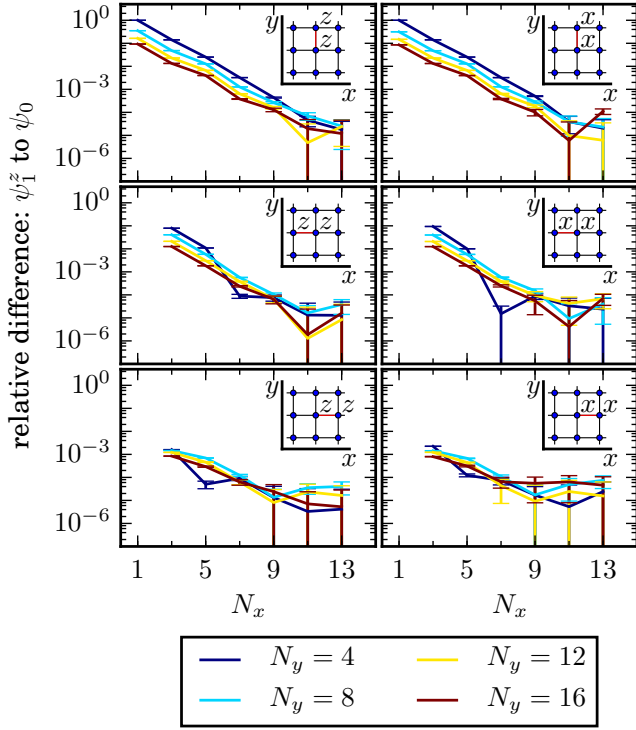


FIG. 3. (Color online) Comparison of nearest-neighbor bulk correlations in ψ_1^z and ψ_0 . The vertical axes show the relative differences $|S_{\psi_1^z}^{bc} - S_{\psi_0}^{bc}|/|S_{\psi_0}^{bc}|$ with $b = c = z$ (left panels) and $b = c = x$ (right panels). Along the horizontal axis, the number of spins in the open direction (N_x) is varied. The different curves correspond to configurations with different N_y . The insets show for which sites the correlation functions were computed. The sites in the central column of the insets correspond to the middle of the cylinder in the x -direction. The relative difference decreases exponentially in N_x .

vanish. Rather, we observe that the differences become stationary if N_y is held fixed and N_x increased. As shown in the right panels of Fig. 4, the differences do, however, tend to zero exponentially as a function of N_y if N_x is chosen large enough.

D. States at a higher level

In the previous subsection, the states at level one in current operators were considered. We also compared spin correlations in ψ_n^a to those in ψ_0 for higher values of n . For very large mode numbers n , only the terms at the edge contribute to the sum in u_{-n}^a . To see this, let

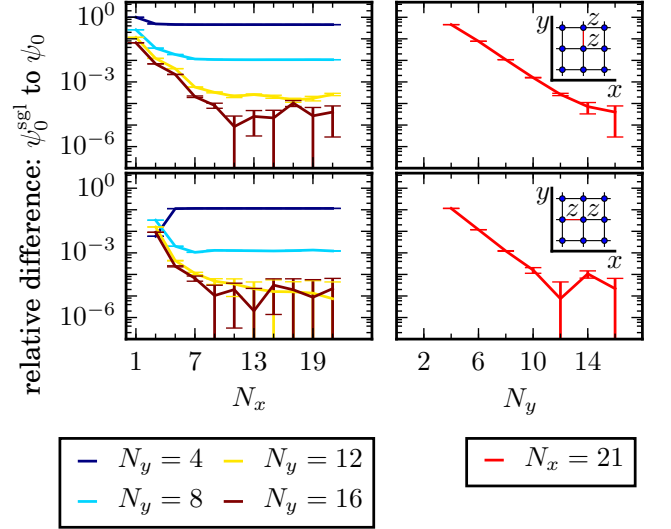


FIG. 4. (Color online) Comparison of nearest-neighbor bulk correlations in ψ_0^{sgl} and ψ_0 . The vertical axes show the relative differences $|S_{\psi_0^{sgl}}^{zz} - S_{\psi_0}^{zz}|/|S_{\psi_0}^{zz}|$. In the left panels, N_x is varied along the horizontal axes and the different curves correspond to different choices of N_y . On the right panels, N_y varies along the horizontal axes and N_x is fixed. For N_x large enough, the differences tend to zero exponentially as a function of N_y .

us consider

$$u_{-n-mN_y}^a = \sum_{j=1}^N \frac{1}{z_j^{n+mN_y}} t_j^a \quad (30)$$

$$\propto \sum_{j_x=1}^{N_x} e^{-\frac{2\pi i}{N_y}(n+mN_y)j_x} \sum_{j_y=1}^{N_y} e^{-\frac{2\pi i}{N_y}n j_y} t_{j_x, j_y}^a. \quad (31)$$

For large values of m , the terms with $j_x > 1$ are exponentially suppressed with respect to those that have $j_x = 1$. We denote the corresponding states with one current operator by χ_n^a :

$$|\chi_n^a\rangle = \lim_{m \rightarrow \infty} |\psi_{n+mN_y}^a\rangle \propto \sum_{j_y=1}^{N_y} e^{-2\pi i \frac{n j_y}{N_y}} t_{1, j_y}^a |\psi_0\rangle. \quad (32)$$

Fig. 5 shows the difference in nearest-neighbor correlations along the y -direction relative to ψ_0 for $N_x = 13$ and $N_y = 8$. The three curves correspond to the states ψ_1^z, ψ_2^z and χ_1^z . As the position in the open direction is increased, the differences vanish exponentially for all three states. We note that the differences are large at the left edge ($i_x = 1$) and small at the right edge ($i_x = 13$). This agrees with the expectation that the operators u_{-n}^a are localized at the left edge. In contrast to the state ψ_0^{sgl} , the states ψ_n^a perturb ψ_0 only at one edge and their behavior is therefore expected to approach that of ψ_0 at the other edge. The results of Fig. 5 provide an indication that ψ_n^a describe edge states also for $n > 1$.

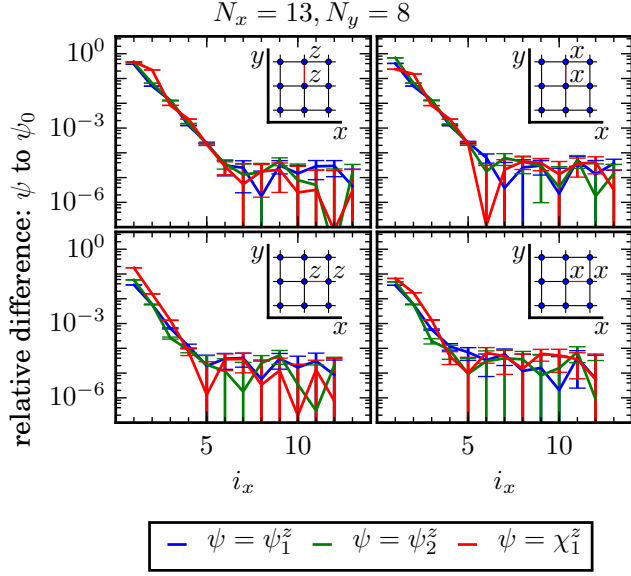


FIG. 5. (Color online) Relative difference $|S_{\psi}^{ab} - S_{\psi_0}^{ab}|/|S_{\psi_0}^{ab}|$ in nearest-neighbor correlators for $\psi \in \{\psi_1^z, \psi_2^z, \chi_1^z\}$ [cf. Eq. (32) for the definition of χ_1^z]. The position i_x in the x -direction is varied along the horizontal axis. The plots in the left panels have $a = b = z$ and those in the right panels $a = b = x$. In the upper panels, the correlations along the y -direction are shown [$j_x = i_x, \Delta_y = 1$] and the lower panels correspond to correlations along the x -direction [$j_x = i_x + 1, \Delta_y = 0$].

We note, however, that the linear span of ψ_n^a for $n \in \{1, \dots, N-1\}$ contains not only edge states. The states ψ_n^a can even be linearly combined so that ψ_0 is perturbed at an arbitrary position j :

$$t_j^a |\psi_0\rangle = \sum_{n=2}^N (\mathcal{Z}^{-1})_{jn} |\psi_{n-1}^a\rangle, \quad (33)$$

where \mathcal{Z} is the matrix defined in Eq. (15). This observation can be understood from the fact that two states ψ_m^a and ψ_n^a are not necessarily orthogonal if $m - n = 0$ modulo N_y . In this case, ψ_m^a and ψ_n^a have the same momentum in the y -direction, as discussed in Sec. III A. The linear combination

$$\begin{aligned} & |\psi_n^a\rangle - e^{-2\pi \frac{N_x-1}{2}} |\psi_{n+N_y}^a\rangle \\ &= \sum_{j_x=1}^{N_x} (1 - e^{-2\pi(j_x-1)}) \sum_{j_y=1}^{N_y} \frac{1}{z_{j_x, j_y}^n} t_{j_x, j_y}^a |\psi_0\rangle, \end{aligned} \quad (34)$$

for example, receives no contribution from spin operators at the left edge ($j_x = 1$). Even though both ψ_n^a and $\psi_{n+N_y}^a$ are perturbed from ψ_0 mostly at $j_x = 1$, this is not the case for the difference of Eq. (34).

E. Inner products of states from current operators

In this subsection, we discuss the relation of inner products between the states $\psi_{n_1 \dots n_1}^{a_1 \dots a_1}$ on the level of the spin system and CFT inner products between states $(J_{-n_1}^{a_1} \dots J_{-n_1}^{a_1})(0)|0\rangle$. For edge states in the continuum that are constructed from descendant states of a CFT, the authors of Ref. 11 come to the remarkable conclusion that, in the thermodynamic limit and under the assumption of exponentially decaying correlations in the bulk, the inner products between edge states are the same as the inner products between CFT states. We now consider inner products between states constructed from current operators to test if a similar correspondence holds for the lattice states $\psi_{n_1 \dots n_1}^{a_1 \dots a_1}$ and the CFT states they are constructed from. The spin system inner products that we consider are given by

$$\begin{aligned} & R^{k+k'} \frac{\langle \psi_{n_1 \dots n_1}^{a_1 \dots a_1} | \psi_{m_1' \dots m_1'}^{b_1' \dots b_1'} \rangle}{\langle \psi_0 | \psi_0 \rangle} \\ & \equiv R^{k+k'} \frac{\langle \psi_0 | (u_{-n_1}^{a_1})^\dagger \dots (u_{-n_l}^{a_l})^\dagger u_{-m_1'}^{b_1'} \dots u_{-m_1'}^{b_1} | \psi_0 \rangle}{\langle \psi_0 | \psi_0 \rangle}, \end{aligned} \quad (35)$$

where N is the number of spins,

$$R = \min_{j \in \{1, \dots, N\}} |z_j| = e^{-\frac{\pi}{N_y}(N_x-1)} \quad (36)$$

is the minimal absolute value of the positions, $k = \sum_{j=1}^l n_j$, and $k' = \sum_{j=1}^{l'} m_j$. The factor $R^{k+k'}$ accounts for the scaling of the operators u_{-n}^a with respect to a rescaling of the positions. The minimal value is chosen because the operators

$$u_{-n}^a = \sum_{j=1}^N \frac{t_j^a}{(z_j)^n} \quad (37)$$

have the highest contribution at the edge with $|z_j| = R$.

We compare the inner products of the lattice system (35) to the CFT inner products

$$\langle 0 | J_{n_1}^{a_1} \dots J_{n_l}^{a_l} J_{-m_1'}^{b_1'} \dots J_{-m_1'}^{b_1} | 0 \rangle. \quad (38)$$

If a correspondence similar to that of Ref. 11 also holds for lattice states, then the expressions of Eq. (35) should approach those of Eq. (38) in the thermodynamic limit.

Note that the inner products of the spin system are hard to evaluate for large system sizes, whereas the CFT inner product can be easily computed using the Kac-Moody algebra (2). On the level of the spin system, the insertion of current operators corresponds to an application of spin operators to ψ_0 [cf. Eq. (12)]. Therefore, the inner products can be determined numerically using a Monte Carlo method if the number of current operators is small.

We calculated the inner products for the states ψ_1^a , ψ_2^a and $\psi_{1,1}^{b,b}$, which are all nonzero states at levels one and

two. For these states, inner products between different states vanish because they have either a different spin or a different momentum. It is thus sufficient to compare the norm squared of a state to the norm squared of the corresponding CFT state, as summarized in the following table:

Spin state	CFT state	Norm squared of CFT state
ψ_1^a	$J_{-1}^a 0\rangle$	$\langle J_{-1}^a J_{-1}^a \rangle = \frac{1}{2}$ (no sum over a)
ψ_2^a	$J_{-2}^a 0\rangle$	$\langle J_{-2}^a J_{-2}^a \rangle = 1$ (no sum over a)
$\psi_{1,1}^{b,b}$	$J_{-1}^b J_{-1}^b 0\rangle$	$\langle J_{-1}^b J_{-1}^b J_{-1}^b J_{-1}^b \rangle = \frac{9}{2}$

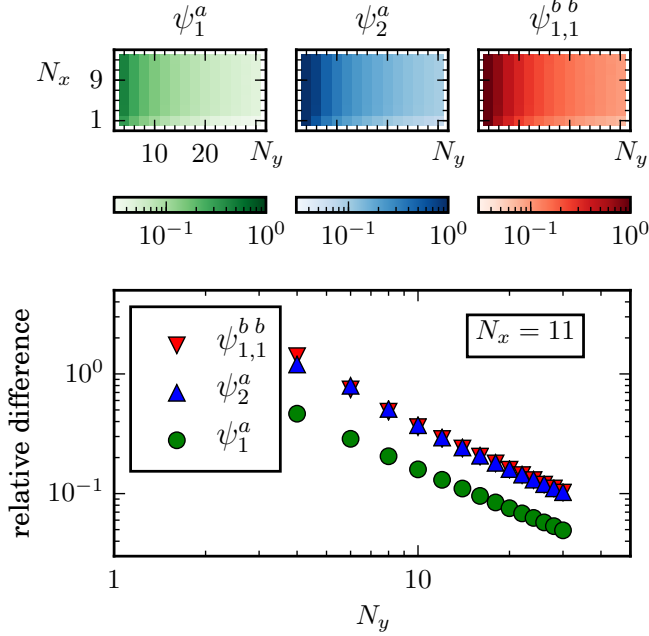


FIG. 6. (Color online) Inner product of spin system states: Relative difference to the CFT expectation [cf. Eq. (39)]. The colors correspond to the states $\psi_{1,1}^{b,b}$ (red), ψ_2^a (blue) and ψ_1^a (green). The upper panels show the relative difference in a color plot as a function of N_x and N_y . We observe a very weak dependence on N_x for $N_x \geq 3$. The lower panel shows the dependence on N_y for $N_x = 11$. For large enough N_y , the data are consistent with a power-law behavior with an exponent of approximately -1.1 . Monte Carlo error bars are not plotted because they are barely visible on the chosen scale. The maximal relative error of the shown data points is 0.31 %.

In Fig. 6, our numerical results are shown for the relative difference

$$\left| \frac{R^{2k} \frac{\langle \psi | \psi \rangle}{\langle \psi_0 | \psi_0 \rangle} - \langle \psi_{\text{CFT}} | \psi_{\text{CFT}} \rangle}{\langle \psi_{\text{CFT}} | \psi_{\text{CFT}} \rangle} \right| \quad (39)$$

as a function of the system size. Here, $\psi \in \{\psi_1^a, \psi_2^a, \psi_{1,1}^{b,b}\}$ is one of the spin states, $k = 1$ for $\psi = \psi_1^a$, $k = 2$ for $\psi \in \{\psi_2^a, \psi_{1,1}^{b,b}\}$, and ψ_{CFT} is the CFT state corresponding to ψ .

For a given system size, we observe a smaller difference for the states at level $k = 1$ than for those at level $k = 2$. The computed inner products approach the CFT expectation if N_y is increased. The dependence on the number of spins in the x -direction is, however, very weak for $N_x \geq 3$. In particular, the CFT result is not approached if N_x is increased and N_y kept fixed. For large enough N_y , our data suggest that the spin system inner products approach the CFT result with a power law in N_y .

IV. LOCAL MODEL HAMILTONIAN

In the previous section, we provided numerical evidence that the states with one current operator insertion represent edge states with respect to ψ_0 . In this section, we study a set of local Hamiltonians on the cylinder. For a suitable choice of parameters, the ground state of the corresponding Hamiltonian has a good overlap with ψ_0 and some of its low-energy excited states are well approximated by ψ_1^a , the states with one current operator of order one.

We study the local Hamiltonians³⁰

$$H = J_2 \sum_{\langle i,j \rangle} t_i^a t_j^a + J'_2 \sum_{\langle\langle i,j \rangle\rangle} t_i^a t_j^a + J_3 \sum_{\langle i,j,k \rangle_{\odot}} \varepsilon_{abc} t_i^a t_j^b t_k^c. \quad (40)$$

In these sums, the sites lie on a square lattice, $\langle i,j \rangle$ denotes all nearest neighbors, $\langle\langle i,j \rangle\rangle$ all next-to-nearest neighbors, and $\langle i,j,k \rangle_{\odot}$ all triangles of nearest neighbors for which i, j , and k are oriented counter-clockwise. It was shown in a previous study³⁰ that the ground state of H on the plane (open boundary conditions in both directions) and on the torus has a good overlap with the KL state for a range of parameters J_2, J'_2 , and J_3 . Here, we study H on a cylinder of size $N_x \times N_y$, where N_x denotes the number of sites in the open direction and N_y the number of sites in the periodical direction. In the following, we parametrize H in terms of two angles θ_1 and θ_2 :

$$\begin{aligned} J_2 &= \cos(\theta_1) \cos(\theta_2), \\ J'_2 &= \sin(\theta_1) \cos(\theta_2), \\ J_3 &= \sin(\theta_2). \end{aligned} \quad (41)$$

For $N_x = 5$ and $N_y = 4$, we studied the overlap between ψ_0 and the ground state ψ_G of H as a function of θ_1 and θ_2 using an exact numerical diagonalization method. We also computed the overlap of the states with one current operator insertion at level one ψ_1^a and the first excited states ψ_E^m of H that have spin one and the same momentum in the y -direction as ψ_1^a . Here, $m \in \{-1, 0, 1\}$ denotes the T^z eigenvalue of ψ_E^m .

We denote the overlap between two states ϕ_1 and ϕ_2 as

$$\Omega(\phi_1, \phi_2) = \frac{|\langle \phi_1 | \phi_2 \rangle|}{\|\phi_1\| \|\phi_2\|}, \quad (42)$$

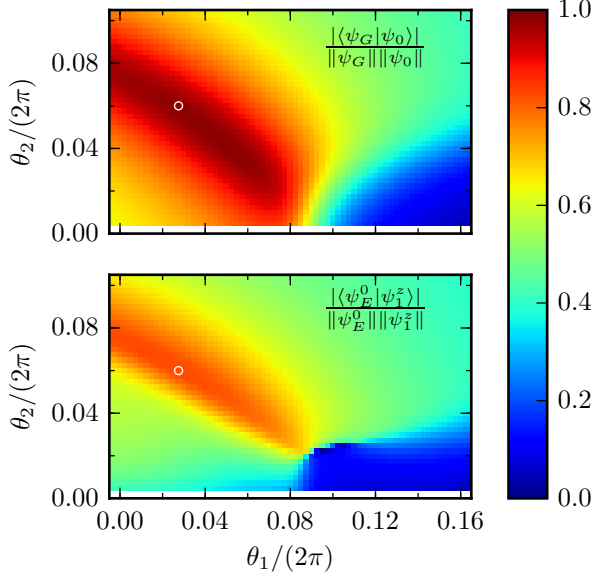


FIG. 7. (Color online) Overlaps of states constructed from CFT and eigenstates of the local Hamiltonian H of Eq. (40) for $N_x = 5$ and $N_y = 4$. The angles θ_1 and θ_2 parametrize the coupling constants of H according to Eq (41). In the upper panel, the overlap $\Omega(\psi_G, \psi_0) \equiv |\langle \psi_G | \psi_0 \rangle| / (\|\psi_G\| \|\psi_0\|)$ between ψ_0 and the ground state ψ_G of H is plotted. The lower panel shows the overlap between ψ_1^z and the first excited state ψ_E^0 of H with the same spin and y -momentum as ψ_1^z [spin one, $T^z = 0$, momentum $3/(8\pi)$]. The point marked with an open circle has $\theta_1 = 0.0275 \times 2\pi$ and $\theta_2 = 0.06 \times 2\pi$ and the highest combined overlap of $\sqrt{\Omega(\psi_G, \psi_0)^2 + \Omega(\psi_E^0, \psi_1^z)^2} \approx 1.2858$.

where $\|\phi\| = \sqrt{\langle \phi | \phi \rangle}$ is the norm of a state. In Fig. 7, the overlaps $\Omega(\psi_G, \psi_0)$ and $\Omega(\psi_E^0, \psi_1^z)$ are shown as a function of the parameters of the Hamiltonian. Due to SU(2) invariance, it is sufficient to consider the overlap between the states ψ_E^0 and ψ_1^z , which both have $T^z = 0$:

$$|\langle \psi_E^1 | \psi_1^+ \rangle| = |\langle \psi_E^{-1} | \psi_1^- \rangle| = |\langle \psi_E^0 | \psi_1^z \rangle|, \quad (43)$$

where $\psi_1^\pm \equiv \psi_1^x \pm i\psi_1^y$. The best value for the combined overlap $\sqrt{\Omega(\psi_G, \psi_0)^2 + \Omega(\psi_E^0, \psi_1^z)^2}$ was obtained for the angles $\theta_1 = 0.0275 \times 2\pi$ and $\theta_2 = 0.06 \times 2\pi$:

$$\frac{\Omega(\psi_G, \psi_0)}{0.9829} \frac{\Omega(\psi_E^0, \psi_1^z)}{0.8289} \frac{\Omega(\psi_G, \psi_0)^{\frac{1}{N}}}{0.9991} \frac{\Omega(\psi_E^0, \psi_1^z)^{\frac{1}{N}}}{0.9907}$$

Since the size of the Hilbert space grows exponentially with the system size N , the overlaps are expected to scale exponentially in N . By taking the N th root, one obtains a measure for the overlap per site, which takes into account this exponential scaling. Notice that the overlap per site is higher than 99 % for both the ground and the excited state.

The low-energy spectrum of H for the parameters with the best overlaps is plotted in Fig. 8. We find 8 energies below the energy of ψ_E^m . The spectra plotted in

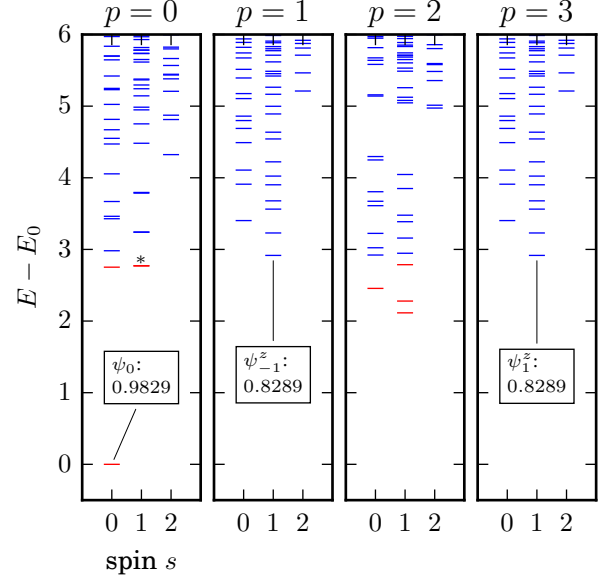


FIG. 8. (Color online) Low energy spectrum of the Hamiltonian H of Eq. (40) for $N_x = 5$, $N_y = 4$, $\theta_1 = 0.0275 \times 2\pi$, and $\theta_2 = 0.06 \times 2\pi$. The ground state energy of H is $E_0 \approx -24.11$. The four panels correspond to the four sectors of y -momentum $p/(2\pi N_y)$ with $p \in \{0, 1, 2, 3\}$. Each shown level has a degeneracy of $2s + 1$ corresponding to the values of T^z . The labels show the ansatz state constructed from CFT and the value for its overlap with the corresponding eigenstate of H . The 8 energies shown in red are those that are smaller than the lowest energy in the $p = 1$ and $p = 3$ sectors. [At the level marked with an asterisk (*), there are actually two energies with a splitting of approximately 1.211×10^{-3} . This is not visible on the scale of the plot.]

Fig. 8 are separated into sectors of different y -momentum $p/(2\pi N_y) = p/(8\pi)$ with $p \in \{0, 1, 2, 3\}$. Note that the states ψ_E^m are the first excited states with $p = 3$. The spectra for the momenta for $p = 1$ and $p = 3$ are the same because H is invariant under the inversion operator \mathcal{I} introduced in Sec. III A:

$$\mathcal{I}^{-1} H \mathcal{I} = H. \quad (44)$$

The relation

$$\mathcal{I}^{-1} \mathcal{T}_y \mathcal{I} = \mathcal{T}_y^{-1} \quad (45)$$

between \mathcal{I} and translation operator in the y -direction \mathcal{T}_y follows directly from their definition (cf. Appendix A 2 and A 3). Therefore, if $|\psi\rangle$ is an eigenstate of H with momentum $p/(2\pi N_y)$, then $\mathcal{I}|\psi\rangle$ is also an eigenstate with momentum $(N_y - p)/(2\pi N_y)$. This means that for $|\psi_E^m\rangle$ with $p = 3$, there is a corresponding eigenstate $\mathcal{I}|\psi_E^m\rangle$ with $p = 1$, which satisfies

$$|\langle \psi_E^0 | \psi_1^z \rangle| = |\langle \mathcal{I} \psi_E^0 | \psi_{-1}^z \rangle|. \quad (46)$$

Here, $|\psi_{-1}^z\rangle = \mathcal{I}|\psi_1^z\rangle$ is the state obtained by inserting the current operator at $z_\infty = \infty$ instead of $z_0 = 0$ [cf. Eq. (20)].

Our results show that the state ψ_0 and the states with one current operator of order one are good approximations of low-energy eigenstates of H for $N_x = 5$, $N_y = 4$, $\theta_1 = 0.0275 \times 2\pi$, and $\theta_2 = 0.06 \times 2\pi$. This raises the question if further eigenstates of H are effectively described by states constructed as CFT correlators. We also computed the overlaps of eigenstates of H with some additional states constructed from current operators for higher orders in current operators. At level two in current operators, the overlaps with the first excited states that have the same spin and momentum as our ansatz states are given by 0.5486 for ψ_2^a (0.9704 per site) and 0.3301 for $\psi_{1,1}^{b,b}$ (0.9461 per site).

In this Section, we considered a local model and computed overlaps between ansatz states constructed from CFT and eigenstates of the model Hamiltonian. In Appendix B, we also derive exact, $SU(2)$ invariant parent Hamiltonians for some of the states constructed from current operators. These Hamiltonians are nonlocal with up to four-body interactions.

V. CONCLUSION

This work studies trial wave functions for lattice FQH states constructed as chiral correlators of the $SU(2)_1$ WZW CFT. To each CFT state, characterized by a sequence of current operators, we associated a corresponding state $\psi_{n_1 \dots n_1}^{a_1 \dots a_1}$ of the lattice system. For continuous systems, analogous states constructed from CFT were proposed as FQH edge states previously^{10,11}. The fact that we work on the lattice allowed us to apply Monte Carlo techniques to test a central expectation for edge states: That the local, bulk properties of different edge states should be the same.

For a system on the cylinder, we compared spin correlation functions in the states with one current operator (ψ_1^a) to the state with no current operators (ψ_0). Our numerical results show that the nearest-neighbor bulk correlations approach each other exponentially as the number of spins in the open direction (N_x) is increased. On the other hand, the states ψ_1^a and ψ_0 are different globally since their spin and momentum are different. This supports the assumption that they describe edge states.

We compared inner products of lattice states at levels one and two in current operators to CFT inner products of the corresponding descendant states. For large enough N_y (periodical direction), the computed inner products approach the CFT expectation with a power law in N_y . This suggests that there is a correspondence between inner products of states $\psi_{n_1 \dots n_1}^{a_1 \dots a_1}$ and CFT inner products in the thermodynamic limit. Such a correspondence was found for continuous wave functions in Ref. 11.

Furthermore, we compared nearest-neighbor bulk correlations in ψ_0^{sgl} to those in ψ_0 , where ψ_0^{sgl} is the singlet component of the state obtained by insertion of two extra primary fields. In contrast to ψ_1^a , we find that the correlations do not approach each other if the thermody-

amic limit is taken only in the open direction. However, if N_x is chosen large enough, the difference in correlation functions vanishes exponentially as a function of N_y .

We showed by an exact diagonalization that ψ_0 has a good overlap with the ground state of a local Hamiltonian and ψ_1^a with the first excited states that have the same spin and momentum as ψ_1^a . This could be an indication that further low-energy excitations of that local Hamiltonian are edge states described by the $SU(2)_1$ WZW CFT. It would be interesting to investigate this relation in more detail for larger system sizes and different topologies.

We showed that the complete Hilbert space is covered by the linear span of the states $\psi_{n_1 \dots n_1}^{a_1 \dots a_1}$ and, therefore, only a subset of these states are edge states. For the states with one current operator, we argued that not all linear combinations of states ψ_m^a describe edge modes because states with the same y -momentum can be non-orthogonal. It is possible to restrict the space of states to an orthogonal subset given by ψ_m^a with $m \in \{1, \dots, N_y\}$.

Taking the limit of large mode numbers could be another possibility of removing bulk states for the linear span of $\psi_{n_1 \dots n_1}^{a_1 \dots a_1}$. More precisely, one can replace n_i by $n_i + m_i N_y$ and then take $m_i \rightarrow \infty$. In this limit, the sum in the operators $u_{-n_i - m_i N_y}^a$ only extends over the edge sites because all other positions are exponentially suppressed. The fact that this class of states (and also linear combinations of such states) is obtained from ψ_0 by application of edge spin operators only, suggests that their complete span represents edge states. For one of these states, χ_1^a , we did numerical tests that indeed indicated that χ_1^a is an edge state.

ACKNOWLEDGMENTS

We acknowledge funding from the EU Integrated Project SIQS, FIS2012-33642, the Comunidad de Madrid grant QUITEMAD+ S2013/ICE-2801 (CAM), the Severo Ochoa Program, and the Villum Foundation.

Appendix A: Translation and inversion of states on the cylinder

1. Transformation under a permutation of the spins

Both the translation operator \mathcal{T}_y and the inversion operator \mathcal{I} act on a product state as a permutation of the spins. Such a permutation operator \mathcal{O}_τ is defined for the permutation τ of N elements as

$$\mathcal{O}_\tau |s_1, \dots, s_N\rangle = |s_{\tau(1)}, \dots, s_{\tau(N)}\rangle. \quad (\text{A1})$$

The action of \mathcal{O}_τ on ψ_0 and $\psi_0^{s_0, s_\infty}$ can be rewritten in terms of a permutation of the positions z_i , which will facilitate our calculations for \mathcal{T}_y and \mathcal{I} . Our derivation of this transformation rule follows Ref. 19.

We consider the wave function

$$\tilde{\psi}_0^{z_1, \dots, z_N}(s_1, \dots, s_N) = \delta_s \chi_s \prod_{i < j}^N (z_i - z_j)^{(s_i s_j + 1)/2}, \quad (\text{A2})$$

which is equivalent to ψ_0 because it only differs by a spin-independent constant [cf. Eq. (8)]. We have also explicitly written out the parametric dependence on the positions z_i . Similarly, the wave function

$$\begin{aligned} & \tilde{\psi}_0^{s_0, s_\infty, z_1, \dots, z_N}(s_1, \dots, s_N) \\ &= \delta_s (-1)^{(1-s_\infty)/2} \chi_s \prod_{n=1}^N z_n^{(s_0 s_n + 1)/2} \\ & \times \prod_{n < m}^N (z_n - z_m)^{(s_n s_m + 1)/2} \end{aligned} \quad (\text{A3})$$

is equivalent to $\psi_0^{s_0, s_\infty}$. Let us first calculate the transformation of $\tilde{\psi}_0^{z_1, \dots, z_N}$ under a simultaneous permutation of both the spins and the coordinates. Since every permutation can be decomposed into a series of transpositions, we consider the case that τ is a transposition:

$$\tau(i) = \begin{cases} i, & \text{if } i \notin \{m, n\}, \\ n, & \text{if } i = m, \\ m, & \text{if } i = n, \end{cases} \quad (\text{A4})$$

for $m, n \in \{1, \dots, N\}$ and $m < n$. It follows that

$$\begin{aligned} & \frac{\tilde{\psi}_0^{z_{\tau(1)}, \dots, z_{\tau(N)}}(s_{\tau(1)}, \dots, s_{\tau(N)})}{\tilde{\psi}_0^{z_1, \dots, z_N}(s_1, \dots, s_N)} \\ &= \underbrace{(-1)^{(n-m)(s_m - s_n)/2}}_{\text{transformation of } \chi_s} \prod_{\substack{i < j, \\ \tau(i) > \tau(j)}}^N (-1)^{(s_{\tau(i)} s_{\tau(j)} + 1)/2} \\ &= (-1)^{(n-m)(s_m - s_n)/2} (-1)^{(s_m s_n + 1)/2} \\ & \times \prod_{j=m+1}^{n-1} (-1)^{(s_j(s_m + s_n) + 2)/2} \\ &= -1. \end{aligned} \quad (\text{A5})$$

Therefore, if τ is a general permutation corresponding to \mathcal{N}_τ subsequent transpositions,

$$\begin{aligned} & \tilde{\psi}_0^{z_{\tau(1)}, \dots, z_{\tau(N)}}(s_{\tau(1)}, \dots, s_{\tau(N)}) \\ &= \text{sign}(\tau) \tilde{\psi}_0^{z_1, \dots, z_N}(s_1, \dots, s_N), \end{aligned} \quad (\text{A6})$$

where $\text{sign}(\tau) = (-1)^{\mathcal{N}_\tau}$ is the signature of the permutation. Substituting s_i by $s_{\tau^{-1}(i)}$ in Eq. (A6), we arrive at the final transformation rule:

$$\begin{aligned} & \tilde{\psi}_0^{z_1, \dots, z_N}(s_{\tau^{-1}(1)}, \dots, s_{\tau^{-1}(N)}) \\ &= \text{sign}(\tau) \tilde{\psi}_0^{z_{\tau(1)}, \dots, z_{\tau(N)}}(s_1, \dots, s_N). \end{aligned} \quad (\text{A7})$$

The transformation under a permutation of the spins can therefore be calculated by considering the corresponding transformation of the coordinates and taking into account the signature of the permutation.

We note that Eq. (A7) is not valid for the original wave function ψ_0 but only for $\tilde{\psi}_0^{z_1, \dots, z_N}$, which differs from ψ_0 by a factor depending on z_i . However, this factor does not depend on the spins. Therefore, if $\tilde{\psi}_0^{z_1, \dots, z_N}$ is an eigenstate of \mathcal{O}_τ , then this is also the case for ψ_0 .

Compared to $\tilde{\psi}_0$, there are some additional factors present the wave function $\tilde{\psi}_0^{s_0, s_\infty, z_1, \dots, z_N}$. Since these are invariant under a permutation of both the spins and the coordinates, a formula analogous to Eq. (A7) holds for $\tilde{\psi}_0^{s_0, s_\infty, z_1, \dots, z_N}$.

2. Translation in the periodical direction

The translation operator \mathcal{T}_y is defined through the permutation $\tilde{\mathcal{T}}_y$:

$$\tilde{\mathcal{T}}_y(i_x, i_y) = \begin{cases} (i_x, i_y + 1), & \text{if } i_y \neq N_y, \\ (i_x, 1), & \text{if } i_y = N_y, \end{cases} \quad (\text{A8})$$

where i_x is the x -component and i_y the y -component of an index i .

The signature of this permutation is given by

$$\text{sign}(\tilde{\mathcal{T}}_y) = (-1)^{N_y(N_y-1)} = (-1)^{N_x}, \quad (\text{A9})$$

where we used that $N = N_y N_x$ is even. In terms of the positions, the transformation corresponds to a multiplication by a phase, $z_{\tilde{\mathcal{T}}_y(j)} = e^{2\pi i/N_y} z_j$. Therefore,

$$\begin{aligned} & \tilde{\psi}_0^{z_1, \dots, z_N}(s_{\tilde{\mathcal{T}}_y^{-1}(1)}, \dots, s_{\tilde{\mathcal{T}}_y^{-1}(N)}) \\ &= \text{sign}(\tilde{\mathcal{T}}_y) \tilde{\psi}_0^{z_{\tilde{\mathcal{T}}_y(1)}, \dots, z_{\tilde{\mathcal{T}}_y(N)}}(s_1, \dots, s_N) \\ &= (-1)^{N_x} \delta_s \chi_s \prod_{i < j}^N \left(e^{2\pi i/N_y} (z_i - z_j) \right)^{(s_i s_j + 1)/2} \\ &= (-1)^{N_x N/2} \tilde{\psi}_0^{z_1, \dots, z_N}(s_1, \dots, s_N). \end{aligned} \quad (\text{A10})$$

Here, we have used that

$$\prod_{i < j}^N e^{\frac{\pi i}{N_y} (s_i s_j + 1)} = (-1)^{N_x \frac{N}{2} + N_x}, \quad (\text{A11})$$

which follows from $\sum_{j=1}^N s_j = 0$. The eigenvalue of ψ_0 with respect to \mathcal{T}_y is therefore $(-1)^{N_x N/2}$. With

$$\mathcal{T}_y u_{-n}^a \mathcal{T}_y^{-1} = e^{-2\pi i n/N_y} u_{-n}^a \quad (\text{A12})$$

it follows that the eigenvalue of $\psi_{n_1 \dots n_l}^{a_1 \dots a_l}$ is $e^{-2\pi i k/N_y} (-1)^{N_x N/2}$, where $k = \sum_{j=1}^l n_j$.

For $\tilde{\psi}_0^{s_0, s_\infty, z_1, \dots, z_N}$, we obtain

$$\begin{aligned} & \tilde{\psi}_0^{s_0, s_\infty, z_1, \dots, z_N}(s_{\tilde{\mathcal{T}}_y^{-1}(1)}, \dots, s_{\tilde{\mathcal{T}}_y^{-1}(N)}) \\ &= (-1)^{N_x} \prod_{n=1}^N e^{\frac{\pi i}{N_y} (s_n s_0 + 1)} \prod_{n < m}^N e^{\frac{\pi i}{N_y} (s_n s_m + 1)} \\ & \times \tilde{\psi}_0^{s_0, s_\infty, z_1, \dots, z_N}(s_1, \dots, s_N) \\ &= (-1)^{N_x + N_x \frac{N}{2}} \tilde{\psi}_0^{s_0, s_\infty, z_1, \dots, z_N}(s_1, \dots, s_N). \end{aligned} \quad (\text{A13})$$

In the last equation, we have used that $\sum_{j=1}^N s_j + s_0 + s_\infty = 0$.

3. Inversion

We require that the inversion \mathcal{I} acts on the positions defined in Eq. (19) as

$$z_{\tilde{\mathcal{I}}(i_x), \tilde{\mathcal{I}}(i_y)} = \frac{1}{z_{i_x, i_y}}. \quad (\text{A14})$$

This leads to the definition

$$\tilde{\mathcal{I}}(i_x, i_y) = \begin{cases} (N_x + 1 - i_x, N_y - i_y), & \text{if } i_y \neq N_y, \\ (N_x + 1 - i_x, N_y), & \text{if } i_y = N_y. \end{cases} \quad (\text{A15})$$

We note that in our choice of z_i , the center of the cylinder is at the unit circle. If this is not the case, then the definition of Eq. (A15) leads to an additional factor when $\tilde{\mathcal{I}}$ is applied to z_i .

In order to determine the sign of the permutation, we arrange the state $|s_1, \dots, s_N\rangle$ in a matrix:

$$|s_{1,1}, \dots, s_{N_x, N_y}\rangle \cong \begin{pmatrix} s_{1,1} & \dots & s_{1,N_y} \\ s_{2,1} & \dots & s_{2,N_y} \\ \vdots & \vdots & \vdots \\ s_{N_x,1} & \dots & s_{N_x, N_y} \end{pmatrix}. \quad (\text{A16})$$

The transformed state is then given by

$$\begin{aligned} & \mathcal{I}|s_{1,1}, \dots, s_{N_x, N_y}\rangle \\ & \cong \begin{pmatrix} s_{N_x, N_y-1} & s_{N_x, N_y-2} & \dots & s_{N_x, 1} & s_{N_x, N_y} \\ s_{N_x-1, N_y-1} & s_{N_x-1, N_y-2} & \dots & s_{N_x-1, 1} & s_{N_x-1, N_y} \\ \vdots & \vdots & \vdots & \vdots & \vdots \\ s_{1, N_y-1} & s_{1, N_y-2} & \dots & s_{1, 1} & s_{1, N_y} \end{pmatrix}. \end{aligned} \quad (\text{A17})$$

To bring the transformed matrix back to the original form, we first reverse all N_y columns and then reverse all N_x rows excluding the last element of each row. A single sequence of L elements can be reversed in $\frac{1}{2}L(L-1)$ steps. Therefore, the sign of the permutation is given by

$$\text{sign}(\tilde{\mathcal{I}}) = (-1)^{N_y \frac{1}{2} N_x (N_x - 1) + N_x \frac{1}{2} (N_y - 1) (N_y - 2)}. \quad (\text{A18})$$

We next determine the contribution from the coordinate part of the wave function ψ_0 . Using Eq. (A14), we

have

$$\begin{aligned} & \tilde{\psi}_0^{z_{\tilde{\mathcal{I}}(1)}, \dots, z_{\tilde{\mathcal{I}}(N)}}(s_1, \dots, s_N) \\ & = \tilde{\psi}_0^{z_1, \dots, z_N}(s_1, \dots, s_N) \prod_{m < n}^N (-z_m z_n)^{-\frac{1}{2}(s_m s_n + 1)} \\ & = \tilde{\psi}_0^{z_1, \dots, z_N}(s_1, \dots, s_N) e^{-\frac{1}{4} \sum_{m \neq n} (s_m s_n + 1) (\log(z_m z_n) + \pi i)} \\ & = \tilde{\psi}_0^{z_1, \dots, z_N}(s_1, \dots, s_N) e^{-\frac{1}{4} \sum_{m, n} (s_m s_n + 1) (\log(z_m z_n) + \pi i)} \\ & \quad \times e^{\frac{1}{2} \sum_i (2 \log(z_i) + \pi i)} \\ & = \tilde{\psi}_0^{z_1, \dots, z_N}(s_1, \dots, s_N) (-1)^{\frac{N}{2} N_x + N_x}. \end{aligned} \quad (\text{A19})$$

In the last step, we have used that $s_1 + \dots + s_N = 0$ and

$$\sum_{n=1}^N \log(z_n) = \pi i (N + N_x). \quad (\text{A20})$$

Therefore, the eigenvalue of ψ_0 with respect to \mathcal{I} is

$$\text{sign}(\tilde{\mathcal{I}}) (-1)^{\frac{N}{2} N_x + N_x} = (-1)^{\frac{N}{2} N_y}. \quad (\text{A21})$$

The states $\psi_{n_1 \dots n_1}^{a_1 \dots a_1}$ are not eigenstates of \mathcal{I} , but transform as

$$\begin{aligned} \mathcal{I}|\psi_{n_1 \dots n_1}^{a_1 \dots a_1}\rangle & = \mathcal{I} u_{-n_1}^{a_1} \mathcal{I}^{-1} \dots \mathcal{I} u_{-n_1}^{a_1} \mathcal{I}^{-1} |\psi_0\rangle \\ & = (-1)^{\frac{N}{2} N_y} u_{n_1}^{a_1} \dots u_{n_1}^{a_1} |\psi_0\rangle. \end{aligned} \quad (\text{A22})$$

Here, we have used that

$$\begin{aligned} \mathcal{I} u_{-n_j}^{a_j} \mathcal{I}^{-1} & = \sum_{i=1}^N \frac{1}{(z_i)^{n_j}} \mathcal{I} t_i^{a_j} \mathcal{I}^{-1} = \sum_{i=1}^N \frac{1}{(z_i)^{n_j}} t_{\tilde{\mathcal{I}}^{-1}(i)}^{a_j} \\ & = \sum_{i=1}^N (z_i)^{n_j} t_i^{a_j} = u_{n_j}^{a_j}, \end{aligned} \quad (\text{A23})$$

if the center of the cylinder is at the unit circle. In terms of the states $\psi_{-n_1 \dots -n_1}^{a_1 \dots a_1}$ defined in Eq. (20), we therefore have

$$\mathcal{I}|\psi_{n_1 \dots n_1}^{a_1 \dots a_1}\rangle = (-1)^{\frac{N}{2} N_y} |\psi_{-n_1 \dots -n_1}^{a_1 \dots a_1}\rangle. \quad (\text{A24})$$

For the transformed states $\mathcal{I}|\psi_{n_1 \dots n_1}^{a_1 \dots a_1}\rangle$, the current operators are therefore inserted at $z_\infty = \infty$ instead of at $z_0 = 0$. Eigenstates of \mathcal{I} with eigenvalues $(\pm 1)(-1)^{\frac{N}{2} N_y}$ are then given by

$$\psi_{n_1 \dots n_1}^{a_1 \dots a_1} \pm \psi_{-n_1 \dots -n_1}^{a_1 \dots a_1}. \quad (\text{A25})$$

Finally, we determine the transformation of $\tilde{\psi}_0^{s_0, s_\infty, z_1, \dots, z_N}$ with respect to \mathcal{I} . As for ψ_0 , there is a contribution from the sign of the permutation and from the transformation of the coordinates. The calculation is similar to that for ψ_0 , only that now $s_0 + s_\infty + \sum_{i=1}^N s_i = 0$. We find

$$\begin{aligned} \mathcal{I}|\tilde{\psi}_0^{s_0, s_\infty, z_1, \dots, z_N}\rangle & = \text{sign}(\tilde{\mathcal{I}}) |\tilde{\psi}_0^{s_0, s_\infty, z_{\tilde{\mathcal{I}}(1)}, \dots, z_{\tilde{\mathcal{I}}(N)}}\rangle \\ & = (-1)^{N_y \frac{N}{2} + N_x + 1} |\tilde{\psi}_0^{s_\infty, s_0, z_1, \dots, z_N}\rangle. \end{aligned} \quad (\text{A26})$$

Since $\psi_0^{s_0, s_\infty}$ and $\tilde{\psi}_0^{s_0, s_\infty, z_1, \dots, z_N}$ only differ by a spin-independent factor, we also have

$$\mathcal{I}|\psi_0^{s_0, s_\infty}\rangle = (-1)^{N_y \frac{N}{2} + N_x + 1} |\psi_0^{s_\infty, s_0}\rangle. \quad (\text{A27})$$

Note that \mathcal{I} exchanges the spins s_0 and s_∞ in $\psi_0^{s_0, s_\infty}$.

Appendix B: Exact parent Hamiltonians

As shown in Sec. IV, the edge states ψ_1^a have a good overlap with low-lying excited states of a local model, for which ψ_0 approximates the ground state. In this section, we analytically construct SU(2)-invariant, nonlocal parent Hamiltonians for some linear combinations of the states $\psi_{n_1 \dots n_l}^{a_1 \dots a_l}$, i.e. Hamiltonians for which they are exact eigenstates with the lowest energy.

1. Construction of parent Hamiltonians

The starting point of our construction is the operator

$$\mathcal{C}^a = \sum_{i \neq j}^N \frac{z_i + z_j}{z_i - z_j} (t_j^a + i\varepsilon_{abc} t_i^b t_j^c). \quad (\text{B1})$$

In Appendix C, we explicitly compute the action of \mathcal{C}^a on states constructed from ψ_0 by insertion of current operators, and show that \mathcal{C}^a does not mix the states $\psi_{n_1 \dots n_l}^{a_1 \dots a_l}$ with different levels $k = \sum_{j=1}^l n_j$ if $k < N_y$. This property is key to our construction of parent Hamiltonians: It allows us to treat the levels separately starting with the lower levels, which have fewer states. The action of \mathcal{C}^a on states at level k is described by a matrix. For low k , the dimension of this matrix is considerably smaller compared to that of an operator acting on the complete Hilbert space. Moreover, the size of the matrix depends only on the level k rather than the number of spins N .

We next add a multiple of the total spin T^a to \mathcal{C}^a and define the operators

$$\mathcal{D}_n^a = \mathcal{C}^a + (n + 1 - N)T^a, \quad (\text{B2})$$

where n is an integer. The operator \mathcal{D}_n^a is also closed in the subspace of states of level k if $k < N_y$ since T^a does not mix states of different levels. For certain values of n , we managed to find states constructed from current operators that are annihilated by the three operators \mathcal{D}_n^a for $a \in \{x, y, z\}$. These states are then ground states of the Hamiltonian

$$H_n = (\mathcal{D}_n^a)^\dagger \mathcal{D}_n^a, \quad (\text{B3})$$

where the index a is summed over. Note that the Hamiltonian H_n is positive semi-definite and SU(2) invariant. H_n is nonlocal and contains terms with up to four-body interactions since \mathcal{D}_n^a has terms linear and quadratic in spin operators.

Before describing our results, we note that the condition $\mathcal{D}_n^a|\psi\rangle = 0$ for all a implies that the state ψ is part of the subspace on which $T^b T^b$ and \mathcal{D}_n^a commute. To show this, we first note that

$$[\mathcal{D}_n^a, T^b] = i\varepsilon_{abc} \mathcal{D}_n^c, \quad (\text{B4})$$

which is a direct consequence of the definitions of Eqs. (B1) and (B2). It then follows that

$$\begin{aligned} [T^b T^b, \mathcal{D}_n^a] |\psi\rangle &= (-i\varepsilon_{bac} T^b \mathcal{D}_n^c - i\varepsilon_{bac} \mathcal{D}_n^c T^b) |\psi\rangle \\ &= -i\varepsilon_{bac} [\mathcal{D}_n^c, T^b] |\psi\rangle = \varepsilon_{bac} \varepsilon_{cbd} \mathcal{D}_n^d |\psi\rangle \\ &= 0, \end{aligned} \quad (\text{B5})$$

where we assumed that $\mathcal{D}_n^a|\psi\rangle = 0$ for all a . The states satisfying $\mathcal{D}_n^a|\psi\rangle = 0$ can therefore be decomposed into sectors of different total spin.

We note that the condition $[T^b T^b, \mathcal{D}_n^a] |\psi\rangle = 0$ is equivalent to

$$[T^b T^b, \mathcal{C}^a + (1 - N)T^a] |\psi\rangle = 0, \quad (\text{B6})$$

since $T^b T^b$ and T^a commute. The operator $\mathcal{C}^a + (1 - N)T^a$ has the advantage that its matrix entries in terms of the states at level k do not depend N and n [cf. Eq. (C8) in Appendix C]. In our calculations, we found it technically easier to first determine the subspace of states on which $T^b T^b$ and $\mathcal{C}^a + (1 - N)T^a$ commute and then look for states that are annihilated by \mathcal{D}_n^a for a suitable n within that subspace.

TABLE II. States constructed from current operators that are annihilated by \mathcal{D}_n^a for $a \in \{x, y, z\}$ on a cylinder with $N_y > k$ [cf. Eqs. (B1) and (B2) for the definition of \mathcal{D}_n^a]. For N_y sufficiently large ($N_y > k$), these states are ground states of the Hamiltonian $H_n = (\mathcal{D}_n^a)^\dagger \mathcal{D}_n^a$.

k State	Spin	n
0 ψ_0	0	any
1 ψ_1^a	1	1
2 —	—	—
3 $\psi_3^a + i\varepsilon_{ade} \psi_{2,1}^{d,e}$	1	5
4 Symmetric-traceless part of $\psi_{3,1}^{a,b}$	2	3
5 $\psi_{3,1,1}^{a,d,d} + \frac{3}{2}i\varepsilon_{ade} \psi_{3,2}^{d,e} + \frac{3}{2}i\varepsilon_{ade} \psi_{4,1}^{d,e} + \frac{9}{4}\psi_5^a$	1	9
6 —	—	—
7 $\psi_{3,3,1}^{a,d,d} + 4\psi_{4,2,1}^{d,a,d} + \frac{5}{3}\psi_{4,2,1}^{a,d,d} + \frac{7}{3}\psi_{5,1,1}^{a,d,d} + i\varepsilon_{ade} \psi_{4,3}^{d,e} + \frac{5}{2}i\varepsilon_{ade} \psi_{5,2}^{d,e} + \frac{9}{2}i\varepsilon_{ade} \psi_{6,1}^{d,e} + \frac{21}{4}\psi_7^a$	1	13
8 Symmetric-traceless part of $i\varepsilon_{ade} \psi_{4,3,1}^{b,d,e} + \frac{1}{2}i\varepsilon_{ade} \psi_{5,2,1}^{b,d,e} - \frac{1}{2}\psi_{5,3}^{a,b} - \psi_{6,2}^{a,b} - 2\psi_{7,1}^{a,b}$	2	7
9 Symmetric-traceless part of $\psi_{5,3,1}^{a,b,c}$	3	5
9 $i\varepsilon_{ade} \psi_{4,3,1,1}^{d,e,f} - \frac{1}{2}\psi_{4,3,2}^{a,d,d} - \frac{3}{2}\psi_{5,2,2}^{a,d,d} - \frac{1}{2}\psi_{4,4,1}^{a,d,d} + 3\psi_{5,3,1}^{d,d,a} - \frac{9}{2}\psi_{5,3,1}^{d,a,d} - \frac{9}{2}\psi_{5,3,1}^{a,d,d} - \frac{9}{2}\psi_{6,2,1}^{d,a,d} - \frac{7}{2}\psi_{6,2,1}^{a,d,d} - 3\psi_{7,1,1}^{a,d,d} - \frac{27}{8}i\varepsilon_{ade} \psi_{5,4}^{d,e} - \frac{21}{8}i\varepsilon_{ade} \psi_{6,3}^{d,e} - \frac{45}{8}i\varepsilon_{ade} \psi_{7,2}^{d,e} - \frac{63}{8}i\varepsilon_{ade} \psi_{8,1}^{d,e} - \frac{105}{8}\psi_9^a$	1	17

We summarize our analytical results in Table II. The states with spin 2 and 3 appear as the symmetric-

traceless parts of states with 2 and 3 open indices, respectively. For a two-index state ϕ^{ab} , the symmetric-traceless part is defined as

$$3(\phi^{ab} + \phi^{ba}) - 2\delta_{ab}\phi^{dd}, \quad (\text{B7})$$

and for a three-index state ϕ^{abc} as³⁴

$$\begin{aligned} & 5(\phi^{abc} + \phi^{bca} + \phi^{cab} + \phi^{cba} + \phi^{bac} + \phi^{acb}) \\ & - 2(\delta_{ab}(\phi^{cdd} + \phi^{dcd} + \phi^{ddc}) + \delta_{ac}(\phi^{bdd} + \phi^{dbd} + \phi^{ddb}) \\ & + \delta_{bc}(\phi^{add} + \phi^{dad} + \phi^{dda})). \end{aligned} \quad (\text{B8})$$

Except for the levels 2 and 6, we find states and corresponding parent Hamiltonians for all levels that were considered. Note that the singlet ψ_0 is a ground state of H_n for any value of n . For the additional ground states, we observe that the value of n tends to be larger at higher levels k . This means that the ground state space of the Hamiltonians H_n with lower n contains states of a lower level in current operators. For example, we only find the ground states ψ_0 and ψ_1^a for H_1 . Similarly, the only appearing ground states of H_3 at levels $k \leq 9$ are ψ_0 and the symmetric-traceless part of $\psi_{3,1}^{a,b}$.

2. Ground-state degeneracies

In the previous subsection, we explicitly constructed analytical ground states of the Hamiltonians H_n with $n \in \{1, 3, 5, 7, 9, 13, 17\}$ in terms of linear combinations of states $\psi_{n_1 \dots n_1}^{a_1 \dots a_1}$ with levels $k \leq 9$. We now study the ground state spaces of the Hamiltonians H_n numerically and provide evidence for $n \in \{1, 3, 5\}$ that the complete ground state space is spanned by the states given in Table II.

TABLE III. Numerically determined ground state multiplets of the Hamiltonians H_n for $n \leq 13$ and an even number of spins N with $N \leq 14$. The second column indicates the minimal number of spins N_y^{\min} in the periodical direction for which the complete shown multiplet was observed in all system with $N_y^{\min} \leq N_y \leq 14$. For a lower number of spins in the y -direction, the observed ground state space is smaller. For even n , we only find a singlet ground state.

n	N_y^{\min}	Ground state multiplet
1	2	$0 \oplus 1$
3	4	$0 \oplus 2$
5	6	$0 \oplus 1 \oplus 3$
7	8	$0 \oplus 2 \oplus 4$
9	10	$0 \oplus 1 \oplus 3 \oplus 5$
11	12	$0 \oplus 2 \oplus 4 \oplus 6$
13	14	$0 \oplus 1 \oplus 3 \oplus 5 \oplus 7$

By an exact diagonalization, we numerically determined the ground state multiplets of the Hamiltonians H_n for $n \leq 13$ and systems with $N = N_x N_y \leq 14$ and N even. Our results are summarized in Table III. We observe that states with spin s occur in the ground state spaces only in systems with $N_y \geq 2s$. Furthermore, we find that the ground state degeneracy does not grow anymore if N_y reaches a certain value N_y^{\min} . This statement is most conclusive for the lower values n , where N_y^{\min} is smaller and we are thus able to probe more systems with $N_y \geq N_y^{\min}$. For $n \in \{1, 3, 5\}$, this implies that all ground states are given by the corresponding states of Table II.

Finally, let us formulate a conjecture about the structure of the states annihilated by \mathcal{D}_n^a , which are ground states of H_n . Our analytical results are consistent with the following rule: For each spin sector $s \in \{1, 2, \dots\}$, there is a series of states at levels $k = s^2 + 2sj$ with $j \in \{0, 1, 2, \dots\}$. These states are annihilated by \mathcal{D}_n^a with $n = 2s - 1 + 4j$. As one can show by induction, the second rule implies that the ground state space of H_n with $n = 2s - 1$ contains the multiplet

$$0 \oplus \begin{cases} 1 \oplus 3 \oplus \dots \oplus s, & \text{if } s \text{ is odd,} \\ 2 \oplus 4 \oplus \dots \oplus s, & \text{if } s \text{ is even.} \end{cases}$$

The numerical results of Table III are consistent with this multiplet structure and thus support the conjecture that the values of n are given by $n = 2s - 1 + 4j$.

Appendix C: Action of \mathcal{C}^a on states built from current operators

Our starting point is the decoupling equation for the states $\psi_{1 \dots 1}^{a_k \dots a_1}$ derived in Ref. 33. This equation describes the action of the operator

$$\mathcal{C}_i^a = \sum_{j \in \{1, \dots, N\} \setminus \{i\}} \frac{z_i + z_j}{z_i - z_j} (t_j^a + i\varepsilon_{abc} t_i^b t_j^c) \quad (\text{C1})$$

on the states $\psi_{1 \dots 1}^{a_k \dots a_1}$ and follows from the CFT null field

$$(K_b^a)_i (J_{-1}^b \phi_{s_i})(z_i) \quad \text{with} \quad (K_b^a)_i = \delta_{ab} - i\varepsilon_{abc} t_i^c. \quad (\text{C2})$$

[The definition of \mathcal{C}_i^a used here differs from that of Ref. 33 by a factor of $2/3$.]

The operator

$$\mathcal{C}^a = \sum_{i=1}^N \mathcal{C}_i^a \quad (\text{C3})$$

was used in Sec. B to construct parent Hamiltonians for states built from current operators.

The decoupling equation reads

$$\begin{aligned} \mathcal{C}_i^a |\psi_1^{a_k \dots a_1}\rangle &= \sum_{q=1}^k \frac{(K_{a_q}^a)_i}{z_i} |\psi_1^{a_k \dots a_{q+1} a_{q-1} \dots a_1}\rangle + (K_b^a)_i T^b |\psi_1^{a_k \dots a_1}\rangle \\ &+ 2(K_b^a)_i \sum_{s_1, \dots, s_N} \sum_{q=2}^k \sum_{n=0}^{q-1} \frac{i\varepsilon_{baqc}}{z_i^{n+1}} \langle \Phi_{\mathbf{s}}(\mathbf{z}) (J_{-1}^{a_k} \dots J_{-1}^{a_{q+1}} J_n^c J_{-1}^{a_{q-1}} \dots J_{-1}^{a_1})(0) \rangle |s_1, \dots, s_N\rangle, \end{aligned} \quad (\text{C4})$$

where

$$\Phi_{\mathbf{s}}(\mathbf{z}) = \phi_{s_1}(z_1) \dots \phi_{s_N}(z_N). \quad (\text{C5})$$

The decoupling equation for the states $\psi_1^{a_k \dots a_1}$, where all mode numbers are one, is enough to describe the action of \mathcal{C}_i^a on states with general mode numbers $\psi_{n_1 \dots n_l}^{a_l \dots a_1}$: Using the Kac-Moody algebra of Eq. (2), the latter can be expressed in terms of the states $\psi_1^{a_k \dots a_1}$ by repeated application of

$$J_{-n}^a = \frac{i}{2} \varepsilon_{abc} [J_{-1}^c, J_{-n+1}^b] \quad (n \neq 0). \quad (\text{C6})$$

On the cylinder, we have

$$\sum_{i=1}^N (z_i)^{-n} = 0, \quad \text{if } n \bmod N_y \neq 0. \quad (\text{C7})$$

Summing over i in Eq. (C4), we therefore obtain for $k < N_y$

$$\begin{aligned} \mathcal{C}^a |\psi_1^{a_k \dots a_1}\rangle &= (N-1) T^a |\psi_1^{a_k \dots a_1}\rangle + \sum_{q=1}^k i\varepsilon_{aqa_c} |\psi_{11}^{ca_k \dots a_{q+1} a_{q-1} \dots a_1}\rangle \\ &+ \sum_{s_1, \dots, s_N} \sum_{q=2}^k \sum_{n=0}^{q-1} G_{a_k \dots a_1}^{q,n}(s_1, \dots, s_N) |s_1, \dots, s_N\rangle, \end{aligned} \quad (\text{C8})$$

with

$$\begin{aligned} G_{a_k \dots a_1}^{q,n}(s_1, \dots, s_N) &= 2 \langle \Phi_{\mathbf{s}}(\mathbf{z}) (J_{-n-1}^{a_q} J_{-1}^{a_k} \dots J_{-1}^{a_{q+1}} J_n^a J_{-1}^{a_{q-1}} \dots J_{-1}^{a_1})(0) \rangle \\ &- 2\delta_{aqa} \langle \Phi_{\mathbf{s}}(\mathbf{z}) (J_{-n-1}^c J_{-1}^{a_k} \dots J_{-1}^{a_{q+1}} J_n^c J_{-1}^{a_{q-1}} \dots J_{-1}^{a_1})(0) \rangle. \end{aligned} \quad (\text{C9})$$

The first two terms on the right hand side of Eq. (C8) are of order k in current operators since

$$T^a |\psi_1^{a_k \dots a_1}\rangle = \sum_{q=1}^k i\varepsilon_{aaqc} |\psi_{11}^{a_k \dots a_{q+1} ca_{q-1} \dots a_1}\rangle. \quad (\text{C10})$$

In the remaining terms, the modes J_n^a and J_n^c can be commuted to the right since $J_n^a|0\rangle = 0$ for $n \geq 0$:

$$(J_n^a J_{-1}^{a_{q-1}} \dots J_{-1}^{a_1})(0)|0\rangle = \sum_{r=1}^{q-1} i\varepsilon_{aa_r d} (J_{-1}^{a_{q-1}} \dots J_{-1}^{a_{r+1}} J_{n-1}^d J_{-1}^{a_{r-1}} \dots J_{-1}^{a_1})(0)|0\rangle, \quad (\text{C11})$$

and similarly for $(J_n^c J_{-1}^{a_{q-1}} \dots J_{-1}^{a_1})(0)|0\rangle$. Iterating this step, the current operator modes with a positive mode number can be eliminated. The resulting terms only have negative mode numbers and are all of order k in current operators.

* benedikt.herwerth@mpq.mpg.de

¹ D. C. Tsui, H. L. Stormer, and A. C. Gossard, “Two-Dimensional Magnetotransport in the Extreme Quantum

- Limit,” Phys. Rev. Lett. **48**, 1559 (1982).
- ² X. G. Wen and Q. Niu, “Ground-state degeneracy of the fractional quantum Hall states in the presence of a random potential and on high-genus Riemann surfaces,” Phys. Rev. B **41**, 9377–9396 (1990).
 - ³ X. G. Wen, “Vacuum degeneracy of chiral spin states in compactified space,” Phys. Rev. B **40**, 7387–7390 (1989).
 - ⁴ X. G. Wen, “Topological Orders in Rigid States,” Int. J. Mod. Phys. B **4**, 239–271 (1990).
 - ⁵ C. W. J. Beenakker, “Edge channels for the fractional quantum Hall effect,” Phys. Rev. Lett. **64**, 216–219 (1990).
 - ⁶ A. H. MacDonald, “Edge states in the fractional-quantum-Hall-effect regime,” Phys. Rev. Lett. **64**, 220–223 (1990).
 - ⁷ X. G. Wen, “Chiral Luttinger liquid and the edge excitations in the fractional quantum Hall states,” Phys. Rev. B **41**, 12838–12844 (1990).
 - ⁸ X. G. Wen, “Electrodynamical properties of gapless edge excitations in the fractional quantum Hall states,” Phys. Rev. Lett. **64**, 2206–2209 (1990).
 - ⁹ X. G. Wen, “Gapless boundary excitations in the quantum Hall states and in the chiral spin states,” Phys. Rev. B **43**, 11025–11036 (1991).
 - ¹⁰ X.-G. Wen, Y.-S. Wu, and Y. Hatsugai, “Chiral operator product algebra and edge excitations of a fractional quantum Hall droplet,” Nucl. Phys. B **422**, 476–494 (1994).
 - ¹¹ J. Dubail, N. Read, and E. H. Rezayi, “Edge-state inner products and real-space entanglement spectrum of trial quantum Hall states,” Phys. Rev. B **86**, 245310 (2012).
 - ¹² K. H. Lee, Z.-X. Hu, and X. Wan, “Construction of edge states in fractional quantum Hall systems by Jack polynomials,” Phys. Rev. B **89**, 165124 (2014).
 - ¹³ G. Moore and N. Read, “Nonabelions in the fractional quantum hall effect,” Nucl. Phys. B **360**, 362–396 (1991).
 - ¹⁴ R. B. Laughlin, “Anomalous Quantum Hall Effect: An Incompressible Quantum Fluid with Fractionally Charged Excitations,” Phys. Rev. Lett. **50**, 1395 (1983).
 - ¹⁵ V. Kalmeyer and R. B. Laughlin, “Equivalence of the resonating-valence-bond and fractional quantum Hall states,” Phys. Rev. Lett. **59**, 2095–2098 (1987).
 - ¹⁶ V. Kalmeyer and R. B. Laughlin, “Theory of the spin liquid state of the Heisenberg antiferromagnet,” Phys. Rev. B **39**, 11879–11899 (1989).
 - ¹⁷ H.-H. Tu, A. E. B. Nielsen, J. I. Cirac, and G. Sierra, “Lattice Laughlin states of bosons and fermions at filling fractions $1/q$,” New J. Phys. **16**, 033025 (2014).
 - ¹⁸ A. E. B. Nielsen, J. I. Cirac, and G. Sierra, “Laughlin Spin-Liquid States on Lattices Obtained from Conformal Field Theory,” Phys. Rev. Lett. **108**, 257206 (2012).
 - ¹⁹ A. E. B. Nielsen and G. Sierra, “Bosonic fractional quantum Hall states on the torus from conformal field theory,” J. Stat. Mech. **2014**, P04007 (2014).
 - ²⁰ N. Metropolis, A. W. Rosenbluth, M. N. Rosenbluth, A. H. Teller, and E. Teller, “Equation of State Calculations by Fast Computing Machines,” J. Chem. Phys. **21**, 1087–1092 (1953).
 - ²¹ D. C. Handscomb, “The Monte Carlo method in quantum statistical mechanics,” Math. Proc. Cambridge Philos. Soc. **58**, 594–598 (1962).
 - ²² D. F. Schroeter, E. Kapit, R. Thomale, and M. Greiter, “Spin Hamiltonian for which the Chiral Spin Liquid is the Exact Ground State,” Phys. Rev. Lett. **99**, 097202 (2007).
 - ²³ R. Thomale, E. Kapit, D. F. Schroeter, and M. Greiter, “Parent Hamiltonian for the chiral spin liquid,” Phys. Rev. B **80**, 104406 (2009).
 - ²⁴ M. Greiter, D. F. Schroeter, and R. Thomale, “Parent Hamiltonian for the non-Abelian chiral spin liquid,” Phys. Rev. B **89**, 165125 (2014).
 - ²⁵ B. Paredes, “Non-Abelian fractional quantum Hall states for hard-core bosons in one dimension,” Phys. Rev. B **85**, 195150 (2012).
 - ²⁶ M. Greiter and R. Thomale, “Non-Abelian Statistics in a Quantum Antiferromagnet,” Phys. Rev. Lett. **102**, 207203 (2009).
 - ²⁷ A. E. B. Nielsen, J. I. Cirac, and G. Sierra, “Quantum spin Hamiltonians for the $SU(2)_k$ WZW model,” J. Stat. Mech. **2011**, P11014 (2011).
 - ²⁸ H.-H. Tu, “Projected BCS states and spin Hamiltonians for the $SO(n)_1$ Wess-Zumino-Witten model,” Phys. Rev. B **87**, 041103 (2013).
 - ²⁹ I. Glasser, J. I. Cirac, G. Sierra, and A. E. B. Nielsen, “Exact parent Hamiltonians of bosonic and fermionic Moore-Read states on lattices and local models,” New J. Phys. **17**, 082001 (2015).
 - ³⁰ A. E. B. Nielsen, G. Sierra, and J. I. Cirac, “Local models of fractional quantum Hall states in lattices and physical implementation,” Nat. Commun. **4**, 2864 (2013).
 - ³¹ V. G. Knizhnik and A. B. Zamolodchikov, “Current algebra and Wess-Zumino model in two dimensions,” Nucl. Phys. B **247**, 83–103 (1984).
 - ³² P. Di Francesco, P. Mathieu, and D. Sénéchal, *Conformal Field Theory*, Graduate Texts in Contemporary Physics (Springer, New York, 1997).
 - ³³ B. Herwerth, G. Sierra, H.-H. Tu, and A. E. B. Nielsen, “Excited states in spin chains from conformal blocks,” Phys. Rev. B **91**, 235121 (2015).
 - ³⁴ A. J. M. Spencer, “A note on the decomposition of tensors into traceless symmetric tensors,” Int. J. Eng. Sci. **8**, 475–481 (1970).